Spacecraft Line-of-Sight Control Using a Single Variable-Speed Control Moment Gyro

Hyungjoo Yoon* and Panagiotis Tsiotras†
Georgia Institute of Technology, Atlanta, Georgia 30332-0150

DOI: 10.2514/1.18777

Complete attitude control of a spacecraft is not possible with only one single-gimbal variable-speed control moment gyro due to the conservation of angular momentum. However, partial attitude control without violating the angular momentum conservation principle is still possible. In this paper feedback controllers using only one single-gimbal variable-speed control moment gyro are presented that drive all three components of the angular velocity of a rigid spacecraft to zero, while at the same time a spacecraft body-axis points along an arbitrary inertial direction. To solve this problem, we first introduce a pair of angles to parametrize all feasible final spacecraft orientations at rest without violating the angular momentum constraint. Based on this parametrization, an LQR control law is designed to locally achieve the control objective. Afterwards, a multistage control law is proposed to achieve the same control objective for large initial conditions.

I. Introduction

RECENT advances in spacecraft and satellite control systems have succeeded in solving several challenging problems dealing with the attitude tracking and stabilization of rigid and flexible spacecraft, including optimal slew maneuvers, precision pointing, formation flying, etc. Techniques from nonlinear, adaptive, optimal, and robust control have been used to this end with great success. Most, if not all, of these results have been developed under the assumption that the spacecraft is actively controlled with a sufficient number of actuators, which is equal to (or even greater than) the number of the degrees of freedom of the system. Although this is certainly the case with most current spacecraft, the issue of controlling a rigid spacecraft with less than three control torques has recently aroused the interest of many researchers, as it provides a theoretical foundation to account for unexpected actuator failures. Minimization of the number of actuators also allows the reduction of the spacecraft weight and even mission cost.

Several papers have been published on the stabilization of the angular velocity vector of a rigid spacecraft to zero with less than three control torques [1–5]. In these works only the kinetic equations are considered, and the objective is to null the angular velocity vector of the spacecraft. Stabilization of the complete equations (kinetics and kinematics) is a much more difficult problem, and it has been addressed in [6–12]. The objective of these references is to stabilize a spacecraft about a desired reference attitude with less than three control torques. See Tsiotras and Doumtchenko [13] for a full survey of the underactuated spacecraft control literature up to the time of its publication. In all the previous references, the control torques are assumed to be provided by some external mechanism (e.g., gas jets or magnetotorquers). Alternatively, internal torques generated by momentum exchange devices, such as reaction or momentum wheels or control moment gyros (CMGs) can be used for spacecraft attitude control. A handful of researchers have worked on the attitude stabilization [14,15], detumbling and/or angular velocity control [16–18] problem using less than three reaction wheels.

Recently, a new alternative for spacecraft attitude control has become available, namely that of a variable-speed control moment gyro (VSCMG). A VSCMG is a hybrid actuator that combines a reaction/momentum wheel (RW/MW) with a single-gimbal control moment gyro [19–23]. Whereas the wheel speed of a conventional CMG is kept constant, the wheel speed of a VSCMG is allowed to vary continuously. Therefore, whereas a RW/MW can generate a torque only along the direction of the wheel spin axis, and a conventional CMG can generate a torque only along the direction that is perpendicular to both the gimbal axis and the spin axis of the CMG at any instant of time, a VSCMG can generate a torque along any direction that lies in the plane perpendicular to the gimbal axis. Hence, a cluster of VSCMGs can generate a torque along an arbitrary direction in the three-dimensional space, as long as at least two or more VSCMGs are used whose gimbal directions are not parallel to each other [20]. Moreover, the extra degree of freedom of a VSCMG (over a conventional RW or CMG) can be used to achieve additional objectives of combined attitude and power tracking control [22] and/or singularity avoidance [21,23]. In fact, VSCMGs are poised to become the actuator of choice for combined attitude control and power management on board orbiting spacecraft. For such applications it is not unusual for the VSCMG wheels to spin at an excess of 40,000 rpm to remain competitive to traditional chemical batteries in terms of energy storage.

Recently, Tsiotras et al. have addressed the angular velocity stabilization of a spacecraft via a single VSCMG actuator [24]. In Marshall and Tsiotras [24], it is shown that complete attitude stabilization may not always be possible due to the angular momentum conservation constraint. Nonetheless, the angular velocity system is linearly controllable, hence stabilizable. Both linear LQR feedback controllers and a nonlinear controller were designed in Richie *et al.* [24] for stabilizing the angular velocity equations to zero.

In the present paper, we provide some new results for the angular velocity stabilization of a spacecraft to zero via a single VSCMG, while achieving at the same time partial attitude control. Even though complete attitude control is not possible due to the momentum conservation constraint as mentioned earlier, it is still possible to achieve stabilization about certain orientations, which all lie in a feasible orientation manifold. We investigate this possibility and provide both linear and nonlinear controllers that locally and semiglobally (as usual, semiglobal stability refers to the type of stability with respect to all initial conditions from an *a posteriori* arbitrarily large set; in contrast to global stability, the controller gains depend on the size of this set) stabilize the angular velocity system.

*Currently with Samsung Electronics Co., Korea; drake.yoon@gmail.com. Student Member AIAA.

†Professor, School of Aerospace Engineering; tsiotras@gatech.edu. Associate Fellow AIAA (corresponding author).

These controllers regulate the spacecraft attitude so that a body-fixed axis (normal to the gimbal axis) aims at a given inertial direction.

The problem under consideration is of interest not only from a theoretical point of view, but also from a practical point of view. For instance, if we install a camera or an antenna fixed on the spacecraft, then we can control the line of sight of this camera/antenna so that it points along a desired direction using a single VSCMG. Therefore, if for a certain mission one does not need to track the complete attitude but one only needs to aim a body-fixed camera or antenna along an arbitrary direction, then a single VSCMG is sufficient to achieve this control objective. Moreover, our study also characterizes the types of missions that are possible when some of the VSCMG actuators used for spacecraft attitude control accidentally fail.

The paper is organized as follows. In Sec. II, we provide the equations of motion of a spacecraft with one VSCMG actuator. We specialize the full dynamic equation of a spacecraft with a cluster of multiple VSCMGs of [22] to the case with a single VSCMG. In Sec. III we investigate all feasible spacecraft orientations, which do not violate the momentum conservation. We subsequently propose a parametrization of all the feasible final orientations of the spacecraft when it is at rest. The control objective is subsequently formulated in terms of this parametrization. In Sec. IV we linearize the system equations about the desired state and we study the controllability of these equations. An LQR feedback controller that locally achieves the control objective is proposed. In Sec. V we design a nonlinear multistage controller that achieves the same control objective from all initial conditions. Finally, numerical examples and simulations that verify the proposed control methodology are presented in Sec. VI.

II.   Equations of Motion

The dynamic equations of motion of a spacecraft with a cluster of VSCMGs have been derived in the literature [19,20,22,25]. Herein, we will use the equations as given by Yoon and Tsiotras [22]. In [22] the equations are derived under the assumptions that the center of mass of each VSCMG wheel coincides with that of the gimbal structure; the spacecraft, wheels, and gimbal structure are rigid; the flywheels and gimbals are balanced; and the spacecraft rotational motion is decoupled from its translational motion. Figure 1 shows a schematic of a spacecraft with a single VSCMG. The body frame $\mathcal{B}$ is represented by the orthonormal set of unit vectors $\hat{\boldsymbol{b}}_1$, $\hat{\boldsymbol{b}}_2$, and $\hat{\boldsymbol{b}}_3$, and its origin is located at the center of mass of the entire spacecraft. The gimbal frame $\mathcal{G}$ is represented by the orthonormal set of unit vectors $\hat{s}$, $\hat{t}$, and $\hat{g}$, and it is located on the gimbal, as shown in Fig. 1. In the developments to follow, and with a slight abuse of notation, we use bold symbols to denote both a vector and its components with respect to a basis. The choice of the basis should be clear from the context. When an ambiguity may be possible we will state the specific choice of the basis used.

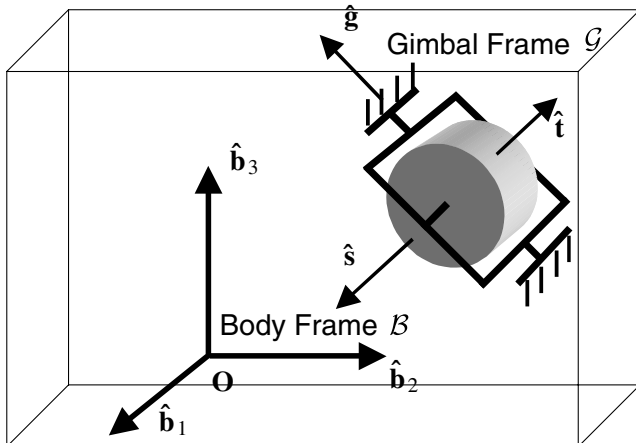Specializing the dynamical equations of motion of [22] to the single VSCMG case, one obtains

Fig. 1   Rigid spacecraft with a single VSCMG.

$$J\dot{\omega} + \dot{J}\omega + I_{cg}\ddot{\gamma}\hat{g} + I_{ws}\Omega\dot{\gamma}\hat{t} + I_{ws}\dot{\Omega}\hat{s} + \omega^{\times}h = 0 \qquad (1)$$

where the total angular momentum vector h of the spacecraft is expressed in the $\mathcal{B}$ frame as

$$h \triangleq J\omega + I_{cg}\dot{\gamma}\hat{g} + I_{ws}\Omega\hat{s} \qquad (2)$$

Here J is the inertia matrix of the whole spacecraft (including the VSCMG), Ω is the wheel spin rate of the VSCMG with respect to the spacecraft, I_{ws} is a moment of inertia of the wheel about its spin axis, and I_{cg} is the sum of the inertia of the wheel and gimbal structure about the gimbal axis. For any vector $v = [v_1, v_2, v_3]^{\mathsf{T}} \in \mathbb{R}^3$, the notation $v^{\times} \in \mathbb{R}^{3\times3}$ represents the equivalent vector cross product operation, that is,

$$v^{\times} \triangleq \begin{bmatrix} 0 & -v_3 & v_2 \\ v_3 & 0 & -v_1 \\ -v_2 & v_1 & 0 \end{bmatrix}$$

The total moment of inertia of the spacecraft will change, in general, as the VSCMG rotates about its gimbal axis, so that the matrix $J = J(\gamma)$ is a function of a gimbal angle γ; see the second term in Eq. (1). However, the dependence of J on γ is weak, especially when the size of spacecraft main body is large. We will therefore assume that J is constant ($\dot{J} = 0$) during controller design. In addition, to simplify the analysis, we assume that the gimbal acceleration term $I_{cg}\ddot{\gamma}\hat{g}$ is ignored. This assumption is standard in the literature [19,20,22,25], and it amounts to rate servo control of the gimbal angle. This is a reasonable simplification because the gimbal angle rate servo control bandwidth is typically high relative to the dynamics of the attitude controllers addressed herein.

Under these assumptions, the dynamic Eq. (1) can be simplified as

$$\begin{aligned} J\dot{\omega} &= -\omega^{\times}h - I_{ws}\Omega\dot{\gamma}\hat{t} - I_{ws}\dot{\Omega}\hat{s} \\ &= -\omega^{\times}(J\omega + I_{cg}\dot{\gamma}\hat{g} + I_{ws}\Omega\hat{s}) - I_{ws}\Omega\dot{\gamma}\hat{t} - I_{ws}\dot{\Omega}\hat{s} \\ &= -\omega^{\times}(J\omega + I_{cg}\dot{\gamma}\hat{g} + I_{ws}\Omega\hat{s}) - I_{ws}\Omega\hat{t}u_1 - I_{ws}\hat{s}u_2 \end{aligned} \qquad (3)$$

where the control input is

$$\begin{bmatrix} u_1 \\ u_2 \end{bmatrix} = \begin{bmatrix} \dot{\gamma} \\ \dot{\Omega} \end{bmatrix} \qquad (4)$$

III.   Feasible Spacecraft Orientations at Rest

A.   Limitations due to Conservation of Angular Momentum

Because the VSCMG is a momentum exchange actuator, the total angular momentum of the spacecraft is conserved (in both magnitude and direction) during a maneuver, assuming no external control/disturbance torques are applied to the spacecraft. This momentum conservation constraint imposes a restriction on the feasible orientations of the spacecraft at rest.

For instance, it is clear that for any given nonzero initial total angular momentum vector H_0, the final rest state of the spacecraft and the VSCMG has to be such that the direction of the spin axis of the VSCMG is aligned with H_0, and the magnitude of the angular momentum of the wheel is equal to the initial magnitude of the angular momentum vector $H_0 \triangleq \| H_0 \|$. That is,

$$H_0 = I_{ws}\Omega_f\hat{s}_f = \mathrm{sgn}\Omega_f H_0\hat{s}_f \qquad (5)$$

where the subscript f denotes the desired final state, when the spacecraft is at rest and $\mathrm{sgn}\Omega_f$ denotes the sign of Ω_f.

Because the final spin axis of the VSCMG is determined by the initial angular momentum H_0, the spacecraft attitude at rest can be determined via only two (Eulerian angle) rotations: one is a rotation of the spacecraft about the body-fixed gimbal axis, and the other is a rotation of the spacecraft about the body axis that coincides with the final spin axis. Since at least three Eulerian angles are needed to express the complete orientation of a spacecraft, one expects that

complete attitude control of the spacecraft is not possible using a single VSCMG; see Marshall and Tsiotras [24] for a formal proof of this claim. As a result, the set of all feasible final spacecraft orientations at rest for a given initial angular momentum $\boldsymbol{H}_0$ can be parametrized by a pair of two angles.

Note that the geometric constraint that the wheel spin axis is aligned with $\boldsymbol{H}_0$ implies that the gimbal axis must be perpendicular to $\boldsymbol{H}_0$, whenever the spacecraft is at rest. Therefore, if we install a camera or an antenna on the spacecraft so that its line of sight is fixed in the plane normal to the gimbal axis, we can aim the camera or antenna at any given inertial direction $\hat{\boldsymbol{n}}$. Before providing a formal proof of the last statement, we present a convenient parametrization of all possible final orientations of the spacecraft when it comes to rest.

B. Parametrization of All Final Feasible Orientations

To this end, let us assume for simplicity that the gimbal axis is fixed along the $\hat{\boldsymbol{b}}_3$ body axis, and the camera/antenna is fixed along the $\hat{\boldsymbol{b}}_1$ body axis, as shown in Fig. 2. The gimbal angle γ is defined as the angle from $\hat{\boldsymbol{b}}_1$ to $\hat{s}$ about the axis $\hat{\boldsymbol{g}} = \hat{\boldsymbol{b}}_3$ in the positive sense. The spin axis of the VSCMG in the body frame can then be written as

$$\hat{s} = \cos\gamma\,\hat{\boldsymbol{b}}_1 + \sin\gamma\,\hat{\boldsymbol{b}}_2 \tag{6}$$

We introduce the following parametrization of the spacecraft orientation. First, we define an inertial frame $\mathcal{H}$ with basis vectors $\hat{\boldsymbol{a}}_1$, $\hat{\boldsymbol{a}}_2$, $\hat{\boldsymbol{a}}_3$, so that the total angular momentum $\boldsymbol{H}_0$ is aligned along $\hat{\boldsymbol{a}}_3$, that is,

$$\hat{\boldsymbol{a}}_3 \triangleq \frac{\boldsymbol{H}_0}{H_0} \tag{7}$$

Given an inertial direction $\hat{\boldsymbol{n}}$ (which is not parallel with $\boldsymbol{H}_0$), we define the remaining two unit vectors by

$$\hat{\boldsymbol{a}}_2 = \frac{\hat{\boldsymbol{a}}_3 \times \hat{\boldsymbol{n}}}{\|\hat{\boldsymbol{a}}_3 \times \hat{\boldsymbol{n}}\|}, \qquad \hat{\boldsymbol{a}}_1 = \hat{\boldsymbol{a}}_2 \times \hat{\boldsymbol{a}}_3 \tag{8}$$

When $\hat{\boldsymbol{n}}$ is parallel to $\boldsymbol{H}_0$, one may define $\hat{\boldsymbol{a}}_1$ and $\hat{\boldsymbol{a}}_2$ arbitrarily as two unit vectors normal to $\hat{\boldsymbol{n}}$, so that the three vectors of $\hat{\boldsymbol{a}}_1, \hat{\boldsymbol{a}}_2, \hat{\boldsymbol{a}}_3$ form an orthonormal set.

A spacecraft orientation can be described by a "3-1-3" body-axis angle sequence from frame $\mathcal{H}$ to frame $\mathcal{B}$ via the direction cosine matrix $R_{\mathcal{H}}^{\mathcal{B}}$ defined as $R_{\mathcal{H}}^{\mathcal{B}} = R_3(\psi)R_1(\theta)R_3(\phi)$, where R_i, for $i = 1, 2, 3$ is the rotational matrix about the ith body axis. Componentwise, we can write

$$R_{\mathcal{H}}^{\mathcal{B}} = \begin{bmatrix} c\phi c\psi - s\phi c\theta s\psi & s\phi c\psi + c\phi c\theta s\psi & s\theta s\psi \\ -c\phi s\psi - s\phi c\theta c\psi & -s\phi s\psi + c\phi c\theta c\psi & s\theta c\psi \\ s\phi s\theta & -c\phi s\theta & c\theta \end{bmatrix} \tag{9}$$
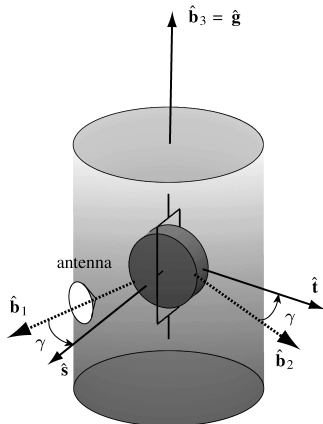
where $\theta \in (0, \pi)$, and ϕ, $\psi \in (-\pi, \pi]$, and $c\phi \triangleq \cos\phi$, $s\phi \triangleq \sin\phi$, etc. From (5–7), one now has

$$\text{sgn}\,\Omega_f \begin{bmatrix} \cos\gamma_f \\ \sin\gamma_f \\ 0 \end{bmatrix} = R_{\mathcal{H}}^{\mathcal{B}}\hat{\boldsymbol{a}}_3 = \begin{bmatrix} \sin\theta_f \sin\psi_f \\ \sin\theta_f \cos\psi_f \\ \cos\theta_f \end{bmatrix} \tag{10}$$

for the case when the spacecraft and the VSCMG gimbal are both at rest. Comparing the third element of (10) yields $\cos\theta_f = 0$, that is, $\theta_f = \pi/2$. Physically, this implies that the only orientations that are accessible at rest are those for which the $\hat{\boldsymbol{b}}_3$ axis (the gimbal axis) is perpendicular to the total angular momentum. Therefore, all feasible spacecraft orientations at rest can be parametrized by the pair of the two remaining Eulerian angles ϕ_f and ψ_f. Since $\theta_f = \pi/2$ it follows that $\sin\theta_f = 1$. Hence $\cos\gamma_f = \text{sgn}\,\Omega_f \sin\psi_f$ and $\sin\gamma_f = \text{sgn}\,\Omega_f \cos\psi_f$. This yields a relation between the final gimbal angle γ_f and the final Eulerian angle ψ_f as follows:

$$\gamma_f = \text{sgn}\,\Omega_f(\pi/2) - \psi_f \tag{11}$$

Equation (11) implies that the final Eulerian angle ψ_f at rest is determined by the final gimbal angle γ_f if the sign of Ω_f is known. Therefore, we can use the gimbal angle γ_f as one of the parameters to describe the spacecraft orientation at rest, in lieu of ψ_f. In the sequel, we denote $\gamma_f^+ = \pi/2 - \psi_f$ and $\gamma_f^- = -\pi/2 - \psi_f = \gamma_f^+ - \pi$.

Next, we provide an algorithm to find the values of the angles ϕ_f and ψ_f (or γ_f) in order to make the line of sight (herein, the $\hat{\boldsymbol{b}}_1$ axis) aim along an arbitrarily given inertial direction $\hat{\boldsymbol{n}}$. To this end, suppose that $\hat{\boldsymbol{n}}$ can be written in the inertial frame $\mathcal{H}$ as $\hat{\boldsymbol{n}} = n_1\hat{\boldsymbol{a}}_1 + n_2\hat{\boldsymbol{a}}_2 + n_3\hat{\boldsymbol{a}}_3$. To make the body axis $\hat{\boldsymbol{b}}_1$ point along the inertial vector $\hat{\boldsymbol{n}}$, we require that

$$\begin{bmatrix} n_1 \\ n_2 \\ n_3 \end{bmatrix} = R_{\mathcal{B}}^{\mathcal{H}}\hat{\boldsymbol{b}}_1 = \begin{bmatrix} \cos\phi_f \cos\psi_f \\ \sin\phi_f \cos\psi_f \\ \sin\psi_f \end{bmatrix} \tag{12}$$

because $\cos\theta_f = 0$ and $\sin\theta_f = 1$. In fact, the right-hand side of (12) is the expression of the vector $\hat{\boldsymbol{n}}$ in the spherical coordinate system, shown in Fig. 3. One can therefore specify the desired final value of the parameters ϕ_f and ψ_f for any given inertial vector $\hat{\boldsymbol{n}}$.

Since $\hat{\boldsymbol{n}}$ is perpendicular to $\hat{\boldsymbol{a}}_2$ it follows that $n_2 = \sin\phi_f \cos\psi_f = 0$. There can be two possibilities for the final required attitude parameters. The first possibility yields $\cos\psi_f = 0$. It follows that $\psi_f = \pm\pi/2$ and $\phi_f \in (-\pi, \pi]$. From (12) it follows that $n_1 = 0$ and thus $n_3 = \pm 1$. This solution is valid only for the special case when the given inertial vector $\hat{\boldsymbol{n}}$ is parallel to $\boldsymbol{H}_0$. The other possibility yields $\sin\phi_f = 0$, which implies that either $\phi_f = 0$ or $\phi_f = \pi$. The former case implies $\cos\psi_f = n_1$ and $\sin\psi_f = n_3$ and hence $\psi_f = \text{atan2}(n_3, n_1)$. The latter case implies $\cos\psi_f = -n_1$ and $\sin\psi_f = n_3$ and hence $\psi_f = \text{atan2}(n_3, -n_1)$. Note that the previous two cases include the case $\cos\psi_f = 0$ as special case.
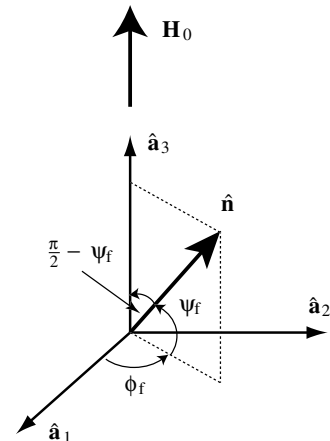

Fig. 2   Axes definition of a spacecraft with a VSCMG and an antenna.

Fig. 3   A desired inertial direction $\hat{\boldsymbol{n}}$ in the inertial frame $\mathcal{H}$.

We have shown that if a camera/antenna line of sight is fixed along the $\hat{\boldsymbol{b}}_1$ axis it can aim along an arbitrary direction $\hat{\boldsymbol{n}}$ when $\omega = 0$. Next, we show that the same is true if the camera/antenna line of sight is anywhere in the plane that is perpendicular to the gimbal axis. In this case we can express the body-fixed unit vector direction of the line of sight of the camera as $\hat{\boldsymbol{b}} = \cos\delta\,\hat{\boldsymbol{b}}_1 + \sin\delta\,\hat{\boldsymbol{b}}_2$, where δ is the angle between $\hat{\boldsymbol{b}}_1$ and $\hat{\boldsymbol{b}}$. Then similarly to Eq. (12), in order to make the body-fixed vector $\hat{\boldsymbol{b}}$ point along the inertial vector $\hat{\boldsymbol{n}}$, we need that

$$
\begin{bmatrix} n_1 \\ n_2 \\ n_3 \end{bmatrix} = R_B^{\mathcal{H}} \hat{\boldsymbol{b}}
$$

$$
= \begin{bmatrix} c\phi_f c\psi_f c\delta + c\phi_f s\psi_f s\delta \\ s\phi_f c\psi_f c\delta + s\phi_f s\psi_f s\delta \\ s\psi_f c\delta - c\psi_f s\delta \end{bmatrix}
$$

$$
= \begin{bmatrix} \cos\phi_f \cos(\psi_f - \delta) \\ \sin\phi_f \cos(\psi_f - \delta) \\ \sin(\psi_f - \delta) \end{bmatrix} \tag{13}
$$

A simple calculation shows that these equations always have a solution, given by

$$
\psi_f = \operatorname{atan2}(n_3, n_1) + \delta, \qquad \phi_f = 0 \tag{14a}
$$

$$
\psi_f = \operatorname{atan2}(n_3, -n_1) + \delta, \qquad \phi_f = \pi \tag{14b}
$$

Next, we show that a camera/antenna must be installed on the spacecraft so that its line-of-sight axis is normal to the gimbal axis in order to aim in an arbitrary inertial direction when $\omega(t_f) = 0$. To this end, let us define a body-fixed unit vector $\hat{\boldsymbol{b}} = b_1\hat{\boldsymbol{b}}_1 + b_2\hat{\boldsymbol{b}}_2 + b_3\hat{\boldsymbol{b}}_3$. When the spacecraft is at rest (and thus $\theta_f = \pi/2$), the vector $\hat{\boldsymbol{b}}$ can be written in the $\mathcal{H}$ frame as $\hat{\boldsymbol{b}} = a_1\hat{\boldsymbol{a}}_1 + a_2\hat{\boldsymbol{a}}_2 + a_3\hat{\boldsymbol{a}}_3$, where

$$
\begin{bmatrix} a_1 \\ a_2 \\ a_3 \end{bmatrix} = R_B^{\mathcal{H}} \hat{\boldsymbol{b}} = \begin{bmatrix} c\phi_f c\psi_f & -c\phi_f s\psi_f & s\phi_f \\ s\phi_f c\psi_f & -s\phi_f s\psi_f & -c\phi_f \\ s\psi_f & c\psi_f & 0 \end{bmatrix} \begin{bmatrix} b_1 \\ b_2 \\ b_3 \end{bmatrix} \tag{15}
$$

To make the $\hat{\boldsymbol{b}}$ axis point along the inertial direction $\hat{\boldsymbol{n}}$, the final Euler angles ϕ_f and ψ_f must be such that $\hat{\boldsymbol{b}} \cdot \hat{\boldsymbol{n}} = a_1 n_1 + a_2 n_2 + a_3 n_3 = 1$. In particular, let us consider the case when the line-of-sight axis (the $\hat{\boldsymbol{b}}$ axis) is commanded so that it aims in the direction of the total angular momentum, that is $\hat{\boldsymbol{n}} = \hat{\boldsymbol{a}}_3 = \boldsymbol{H}_0/H_0$. Then, $\hat{\boldsymbol{b}} \cdot \hat{\boldsymbol{n}} = \hat{\boldsymbol{b}} \cdot \hat{\boldsymbol{a}}_3 = a_3 = b_1 s\psi_f + b_2 c\psi_f = \sqrt{b_1^2 + b_2^2}$ $\sin(\psi_f + \alpha)$, where $\cos\alpha = b_1/\sqrt{b_1^2 + b_2^2}$, $\sin\alpha = b_2/\sqrt{b_1^2 + b_2^2}$. Because $\hat{\boldsymbol{b}} \cdot \hat{\boldsymbol{n}} = 1$ it follows that $b_1^2 + b_2^2 = 1$, and thus $b_3 = 0$, which implies that the body-fixed vector $\hat{\boldsymbol{b}}$ must be perpendicular to the gimbal axis $\hat{\boldsymbol{b}}_3 = \hat{\boldsymbol{g}}$. We have thus proved the following:

Proposition 1: Assume that $\boldsymbol{H}_0 \neq 0$. We can point any body-fixed axis of a spacecraft with a single VSCMG along an arbitrary inertial direction if and only if this axis lies in the plane that is normal to the VSCMG gimbal axis.

Hereafter, for simplicity, we will consider only the case of $\delta = 0$, that is $\hat{\boldsymbol{b}} = \hat{\boldsymbol{b}}_1$. Figure 4 shows two final rest configurations for which $\hat{\boldsymbol{b}}_1$ points along the given inertial direction $\hat{\boldsymbol{n}}$ for the case when $\phi_f = 0$. There are two possible cases, as expected from Eq. (11). One is with a positive final wheel speed $\Omega_f = \Omega_f^+ \triangleq H_0/I_{ws} > 0$. In this case, the final gimbal axis $\hat{\boldsymbol{s}}_f$ is aligned along $\boldsymbol{H}_0$ in the same direction, as shown in Fig. 4a. The other case is with a negative final wheel speed, that is, $\Omega_f = \Omega_f^- \triangleq -H_0/I_{ws} < 0$. The final spin axis $\hat{\boldsymbol{s}}_f$ is aligned along $\boldsymbol{H}_0$ but has the opposite direction, as shown in Fig. 4b. In both cases, the final $\hat{\boldsymbol{b}}_1$ axis points in the direction of $\hat{\boldsymbol{n}}$, as desired. Notice that the gimbal axis $\hat{\boldsymbol{g}} = \hat{\boldsymbol{b}}_3$ is perpendicular to the total angular momentum vector $\boldsymbol{H}_0 = H_0\hat{\boldsymbol{a}}_3$ because $\theta_f = \pi/2$.

a) $\Omega_f = \Omega_f^+ > 0.$ b) $\Omega_f = \Omega_f^- < 0.$
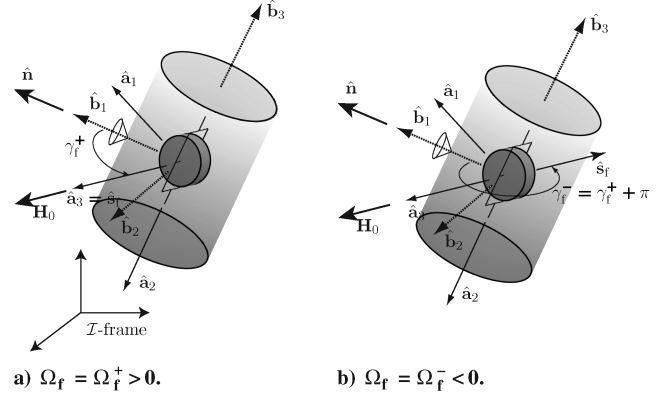
Fig. 4 Desired attitudes with $\omega = 0$ for given H_0 and $\hat{n}$; case when $\phi_f = 0$.

a) $\Omega_f = \Omega_f^+ > 0.$ b) $\Omega_f = \Omega_f^- < 0.$
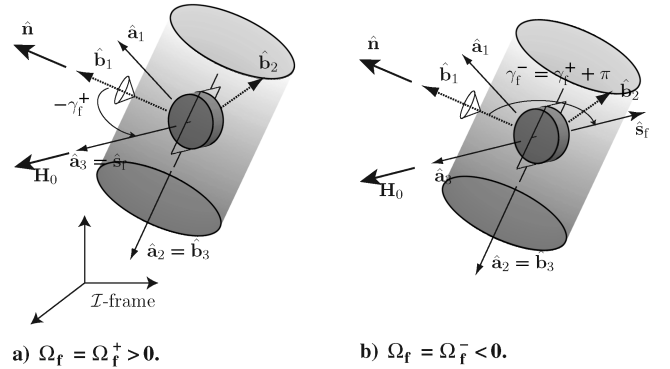
Fig. 5 Desired attitudes with $\omega = 0$ for given H_0 and $\hat{n}$; case when $\phi_f = \pi$.

Figure 5 shows two final rest configurations for which $\hat{\boldsymbol{b}}_1$ points in the given inertial direction $\hat{\boldsymbol{n}}$ for the case $\phi_f = \pi$. Similarly, with the case with $\phi_f = 0$, there are two possible configurations depending on the sign of the final wheel speed Ω_f. Figures 5a and 5b show the final desired orientation of the spacecraft with $\Omega_f > 0$ and $\Omega_f < 0$, respectively.

For either case, $\phi_f = 0$ or $\phi_f = \pi$, the final gimbal angle γ_f is computed from Eqs. (11). Specifically, we have

$$
\cos\gamma_f^+ = \cos\left(\frac{\pi}{2} - \psi_f\right) = \sin\psi_f = n_3 = \frac{\boldsymbol{H}_0 \cdot \hat{\boldsymbol{n}}}{H_0} \tag{16}
$$

and similarly for γ_f^-.

For each value of the sign of Ω_f the pair (ϕ_f, γ_f) determines the final spacecraft orientation at rest. Furthermore, if we design a controller that achieves

$$
\omega \to 0 \tag{17a}
$$

$$
\gamma_e \triangleq \gamma - \gamma_f \to 0 \tag{17b}
$$

$$
\phi_e \triangleq \phi - \phi_f \to 0 \tag{17c}
$$

then the spacecraft will be brought to rest and the $\hat{\boldsymbol{b}}_1$ axis will point along the desired inertial direction $\hat{\boldsymbol{n}}$. Hereafter, for simplicity, we consider only the cases corresponding to $\phi_f = 0$. The case with $\phi_f = \pi$ can be treated similarly. Also, notice that when $\hat{\boldsymbol{n}}$ is parallel to

H_0 the controller does not need to meet the last requirement in (17) because (17c) is redundant in this case and thus it can be ignored.

IV. Linearized System Analysis and Controller Design

The kinematic differential equation for the "3-1-3" rotational sequence is given by

$$\begin{bmatrix} \dot{\phi} \\ \dot{\theta} \\ \dot{\psi} \end{bmatrix} = \frac{1}{\sin\theta} \begin{bmatrix} s\psi & c\psi & 0 \\ c\psi s\theta & -s\psi s\theta & 0 \\ -s\psi c\theta & -c\psi c\theta & s\theta \end{bmatrix} \begin{bmatrix} \omega_1 \\ \omega_2 \\ \omega_3 \end{bmatrix} \quad (18)$$

and the differential equation of γ_e is

$$\dot{\gamma}_e = \dot{\gamma} = u_1. \quad (19)$$

In this section, we linearize the nonlinear equations of motion, given by (3), (18), and (19). We then use these equations to investigate the controllability properties of the system $(\omega, \gamma_e, \phi_e)$. We also present an LQR control law that satisfies the control objectives (17) and thus stabilizes the angular velocity of spacecraft with a body-fixed axis aiming at a given inertial direction.

A. Controllability Analysis

The desired equilibrium points of Eqs. (3), (18), and (19) are given by $\omega = 0$, $\gamma_e = 0$, $\phi_e = 0$, $\Omega = \Omega_f$ and $u = [u_1, u_2]^\mathsf{T} = 0$. Moreover, we know that $\sin\theta \approx 1$, $\sin\psi \approx \mathrm{sgn}\Omega_f \cos\gamma$ and $\cos\psi \approx \mathrm{sgn}\Omega_f \sin\gamma$ near the equilibrium. Thus, one can linearize the differential equation of ϕ_e as follows:

$$\dot{\phi}_e = \dot{\phi} \approx (\omega_1 \cos\gamma_f + \omega_2 \sin\gamma_f)\mathrm{sgn}\Omega_f = \omega^\mathsf{T}\hat{s}_f \mathrm{sgn}\Omega_f \quad (20)$$

The linearized equations can be written as [24]

$$\begin{bmatrix} \dot{\omega} \\ \dot{\gamma}_e \\ \dot{\phi}_e \end{bmatrix} = \begin{bmatrix} A_1 & 0 & 0 \\ 0 & 0 & 0 \\ A_2 & 0 & 0 \end{bmatrix} \begin{bmatrix} \Delta\omega \\ \gamma_e \\ \phi_e \end{bmatrix} + \begin{bmatrix} B_1 & B_2 \\ 1 & 0 \\ 0 & 0 \end{bmatrix} \begin{bmatrix} u_1 \\ \mathrm{sgn}\Omega_f u_2 \end{bmatrix} \quad (21)$$

where,

$$A_1 \triangleq J^{-1} I_{\mathrm{ws}} \Omega_f \hat{s}_f^\times \quad (22a)$$

$$A_2 \triangleq \hat{s}_f^\mathsf{T} \mathrm{sgn}\Omega_f \quad (22b)$$

$$B_1 \triangleq -J^{-1} I_{\mathrm{ws}} \Omega_f \hat{t}_f \quad (22c)$$

$$B_2 \triangleq -J^{-1} I_{\mathrm{ws}} \hat{s}_f \quad (22d)$$

where all vectors are expressed in the $\mathcal{B}$ frame.

Proposition 2: The linearized system described by Eqs. (21) and (22) is controllable for any $\gamma_f \in [0, 2\pi)$ and $\Omega_f \neq 0$.

Proof. The controllability of Eqs. (21) and (22) can be shown using the Popov–Belevitch–Hautus (PBH) test [[26], p. 135]. A necessary and sufficient condition for the controllability of (21) and (22) is that the matrix $\mathcal{C}(\lambda)$ defined as

$$\mathcal{C}(\lambda) \triangleq \begin{bmatrix} A_1 - \lambda I & 0 & 0 & B_1 & B_2 \\ 0 & -\lambda & 0 & 1 & 0 \\ A_2 & 0 & -\lambda & 0 & 0 \end{bmatrix} \quad (23)$$

has rank 5 for all complex $\lambda \in \mathbb{C}$. It can be easily proved using the approach of [24] that the linearized subsystem (ω, γ_e) is controllable, that is, the pair of matrices $(\bar{A}, \bar{B})$, where

$$\bar{A} \triangleq \begin{bmatrix} A_1 & 0 \\ 0 & 0 \end{bmatrix}, \qquad \bar{B} \triangleq \begin{bmatrix} B_1 & B_2 \\ 1 & 0 \end{bmatrix} \quad (24)$$

is controllable [27]. Therefore, it follows easily that rank $\mathcal{C}(\lambda) = 5$ for all $\lambda \neq 0$. We only need to check the rank of the matrix

$$\mathcal{C}'(0) \triangleq \begin{bmatrix} A_1 & B_1 & B_2 \\ 0 & 1 & 0 \\ \hat{s}_f^\mathsf{T} \mathrm{sgn}\Omega_f & 0 & 0 \end{bmatrix} \quad (25)$$

Notice that

$$\mathrm{rank}\, \mathcal{C}'(0) = \mathrm{rank} \begin{bmatrix} \hat{s}_f^\times & \hat{t}_f & \hat{s}_f \\ 0 & 1 & 0 \\ \hat{s}_f^\mathsf{T} & 0 & 0 \end{bmatrix} \quad (26)$$

To this end, assume that there exist a vector $v_1 \in \mathbb{R}^3$, and scalars $v_2, v_3 \in \mathbb{R}$ such that

$$\begin{bmatrix} v_1^\mathsf{T} & v_2 & v_3 \end{bmatrix} \begin{bmatrix} \hat{s}_f^\times & \hat{t}_f & \hat{s}_f \\ 0 & 1 & 0 \\ \hat{s}_f^\mathsf{T} & 0 & 0 \end{bmatrix} = 0 \quad (27)$$

Equivalently,

$$v_1^\mathsf{T} \hat{s}_f^\times + v_3 \hat{s}_f^\mathsf{T} = 0 \quad (28)$$

$$v_1^\mathsf{T} \hat{t}_f^\times + v_2 = 0 \quad (29)$$

$$v_1^\mathsf{T} \hat{s}_f = 0 \quad (30)$$

Equation (28) holds if and only if $v_1 = 0$ and $v_3 = 0$. From (29) it follows that $v_2 = 0$. This implies that the left null space of the matrix in Eq. (27) contains only the zero vector and thus rank $\mathcal{C}'(0) = 5$ and the proof is completed.

Notice that proposition 2 does not ensure the controllability of the linearized system if $\Omega_f = 0$. However, if the initial angular momentum H_0 is not zero, then $\Omega_f \neq 0$ by conservation of the angular momentum.

B. Linear Control Design

In this section we outline briefly the design of a linear controller via LQR theory for the linearized system (21). Let the matrices A and B denote the system matrices in Eq. (21). Then we can determine a control gain matrix $K \in \mathbb{R}^{2\times5}$ such that the static full-state feedback law

$$u = [u_1, \mathrm{sgn}\Omega_f u_2]^\mathsf{T} = -K[\omega^\mathsf{T}, \gamma_e, \phi_e]^\mathsf{T} \quad (31)$$

minimizes the performance index

$$\mathcal{J} \triangleq \int_0^\infty (x^\mathsf{T} Q x + u^\mathsf{T} R u)\, \mathrm{d}t \quad (32)$$

where $x = [\omega^\mathsf{T}, \gamma_e, \phi_e]^\mathsf{T}$, $Q \in \mathbb{R}^{5\times5}$ is a positive semidefinite matrix, and $R \in \mathbb{R}^{2\times2}$ is a positive definite matrix. The gain matrix K is computed by $K = R^{-1}B^\mathsf{T}P$, where P is the solution of the algebraic Riccati equation (ARE)

$$A^\mathsf{T}P + PA - PBR^{-1}B^\mathsf{T}P + Q = 0 \quad (33)$$

No further details are provided because LQR theory is well known in the literature [28].

V. Nonlinear System Analysis and Controller Design

The LQR controller of the previous section ensures asymptotic stability only locally about the equilibrium $\omega = 0$ (and thus also $\Omega = \Omega_f$), $\gamma_e = 0$ and $\phi_e = 0$. In realistic cases, however, one cannot expect that the initial states will be near the equilibrium point. To achieve the desired stabilization objective for all initial conditions at large (not necessarily close to the origin), it is necessary to design a controller based on the complete nonlinear equations of motion.

In the sequel we suggest a control methodology that comprises a sequence of three stages. At the first stage, only the angular velocity ω is controlled in order to decrease its value toward zero. When a certain condition is met, the controller switches to the second stage in which both ω and the gimbal angle γ are controlled to their desired values, according to the sign of the wheel speed. Once ω and γ are sufficiently close to the values at the desired equilibrium, then the controller switches to the third stage where the LQR controller designed in Sec. IV regulates the Euler angle ϕ to ϕ_f, along with ω and γ.

The following assumptions are made in order to simplify the analysis.

Assumption 1: The spacecraft is inertially axisymmetric about the gimbal axis $\hat{g} = \hat{b}_3$.

Assumption 2: The spacecraft is not inertially symmetric.

Under assumption 1, the inertia matrix written in the gimbal frame $\mathcal{G}$ takes the form

$$J = \begin{bmatrix} J_t & 0 & 0 \\ 0 & J_t & 0 \\ 0 & 0 & J_a \end{bmatrix} \qquad (34)$$

Assumption 2 implies that $J_t \neq J_a$.

A. Angular Velocity Stabilization

Consider the positive definite, continuously differentiable Lyapunov function candidate

$$V_1(\omega) = \tfrac{1}{2}\omega^\mathsf{T} J\omega \qquad (35)$$

Its time derivative along the trajectories of the system (3) yields

$$\dot{V}_1 = \omega^\mathsf{T} J\dot{\omega} = \omega^\mathsf{T}[-\omega^\times (J\omega + I_{cg}\dot{\gamma}\hat{g} + I_{ws}\Omega\hat{s}) - I_{ws}\Omega\hat{t}u_1 \\ - I_{ws}\hat{s}u_2] = -\omega_t I_{ws}\Omega u_1 - I_{ws}\omega_s u_2 \qquad (36)$$

where $\omega_s = \omega^\mathsf{T}\hat{s}$ and $\omega_t = \omega^\mathsf{T}\hat{t}$ are the projections of the body angular velocity ω along the spin and transverse axes of the gimbal frame, respectively, that is, $\omega = \omega_s\hat{s} + \omega_t\hat{t} + \omega_g\hat{g}$, where $\omega_g = \omega^\mathsf{T}\hat{g}$. Taking a control law as

$$u_1 = \dot{\gamma} = k_1\omega_t I_{ws}\Omega, \qquad k_1 > 0 \qquad (37a)$$

$$u_2 = \dot{\Omega} = k_2 I_{ws}\omega_s, \qquad k_2 > 0 \qquad (37b)$$

yields

$$\dot{V}_1 = -k_1(\omega_t I_{ws}\Omega)^2 - k_2(I_{ws}\omega_s)^2 \leq 0 \qquad (38)$$

To show that the control law (37) provides an asymptotically stabilizing feedback, we need to show that there exists $c_0 > 0$ such that, for each $c_1 \in (0, c_0)$, no trajectory of the vector field with $u_1 = u_2 = 0$ is contained inside the set

$$\mathcal{L}_c \triangleq \{\omega: V_1(\omega) = c_1 \text{ and } \omega_t I_{ws}\Omega = I_{ws}\omega_s = 0\} \qquad (39)$$

In other words, we need to show that no trajectories of the control-free system stay in nontrivial invariant sets of $\dot{V}_1 = 0$, which are characterized by the equations

$$\omega_t I_{ws}\Omega = 0 \qquad (40a)$$

$$I_{ws}\omega_s = 0 \qquad (40b)$$

Inside the invariant set $\mathcal{L}_c$, we have that $u_1 = \dot{\gamma} = 0$ and $u_2 = \dot{\Omega} = 0$, and thus γ and Ω are constant. In addition, $\omega_s = 0$ from (40b). Because γ is constant, the gimbal frame $\mathcal{G}$ is fixed in the body frame. Rewriting the dynamic equations in the $\mathcal{G}$ frame, one obtains

$$J\dot{\omega} = -\omega^\times(J\omega + I_{ws}\Omega\hat{s}) = -\omega^\times h \qquad (41)$$

where

$$\omega = [0, \omega_t, \omega_g]^\mathsf{T}, \qquad \dot{\omega} = [0, \dot{\omega}_t, \dot{\omega}_g]^\mathsf{T} \qquad (42)$$

Using Eqs. (34) and (42), Eq. (41) can be written as

$$\begin{bmatrix} 0 \\ J_t\dot{\omega}_t \\ J_a\dot{\omega}_g \end{bmatrix} = - \begin{bmatrix} h_3\omega_t - h_2\omega_g \\ h_1\omega_g \\ -h_1\omega_t \end{bmatrix} = \begin{bmatrix} \omega_t\omega_g(J_t - J_a) \\ -I_{ws}\Omega\omega_g \\ I_{ws}\Omega\omega_t \end{bmatrix} \qquad (43)$$

where

$$h = [h_1, h_2, h_3]^\mathsf{T} = [I_{ws}\Omega, J_t\omega_t, J_a\omega_g]^\mathsf{T} \qquad (44)$$

is the total angular momentum of the vehicle expressed in the gimbal frame. Comparing the first element in Eq. (43), one obtains $\omega_t\omega_g = 0$ for the equilibria. Also, one has $\omega_t\Omega = 0$ from Eq. (40a). Thus, there are two different types of the equilibria:

1) $\omega_t = 0, \omega_g \in \mathbb{R}$: Comparing the second element in Eq. (43), one has $\Omega\omega_g = 0$. If $\omega_g = 0$, then $\omega = 0$, which is the desired equilibrium. However, there can still be a nontrivial equilibrium given by $\Omega = 0, \omega = [0, 0, \pm H_0/J_a]^\mathsf{T}$.

2) $\omega_g = \Omega = 0, \omega_t \in \mathbb{R}$: There can be a nontrivial equilibrium at $\Omega = 0, \omega = [0, \pm H_0/J_t, 0]^\mathsf{T}$.

Therefore, there exist nontrivial equilibria contained inside the invariant set $\mathcal{L}_c$, thus global stabilization is not guaranteed. Nonetheless, these nontrivial equilibria are unstable; see Appendix A for the proof. Therefore, "essentially global stability" or "regional stability" [global stability except a set of negligible size (in mathematical language, a set of measure zero)] follows. This type of stability is all that is needed from a practical point of view.

B. Stabilization of ω, γ_e, and Ω_e

The nonlinear controller designed in the previous section stabilizes ω, but it cannot achieve the overall control objective, as it controls only the angular velocity vector. Hence, the final orientation of the spacecraft is not controlled. In this section, we design a nonlinear controller which makes, in addition to $\omega \to 0$, also $\gamma_e = \gamma - \gamma_f \to 0$.

Notice that there are two possible desired values of the final gimbal angle γ_f in this case, depending on the sign of the final wheel speed Ω_f, as shown in Eq. (11) or Eq. (16). The magnitude of the final wheel speed is given by $|\Omega_f| = H_0/I_{ws}$ as $\omega \to 0$ due to the momentum conservation law, but its sign can be either positive or negative, unless it is explicitly controlled. Thus, we also need to control the wheel speed Ω as well as ω and γ.

First, let us consider a nonlinear controller which makes $\omega \to 0$, $\gamma \to \gamma_f^+$ and $\Omega \to \Omega_f^+$. For this purpose, define a Lyapunov function candidate $V_2^+(\omega, \gamma_e, \Omega_e^+)$ as

$$V_2^+(\omega, \gamma_e^+, \Omega_e^+) \triangleq \tfrac{1}{2}\omega^\mathsf{T} J\omega + \tfrac{1}{2}k_\gamma\gamma_e^{+2} + \tfrac{1}{2}k_\Omega\Omega_e^{+2} \\ = \tfrac{1}{2}(J_t(\omega_s^2 + \omega_t^2) + J_a\omega_g^2) + \tfrac{1}{2}k_\gamma\gamma_e^{+2} + \tfrac{1}{2}k_\Omega\Omega_e^{+2}, \\ k_\gamma, k_\Omega > 0 \qquad (45)$$

where $\gamma_e^+ \triangleq \gamma - \gamma_f^+$ and $\Omega_e^+ \triangleq \Omega - \Omega_f^+$. Its time derivative along the trajectories of the system (3) and (19) yields

$$\dot{V}_2^+ = \omega^\mathsf{T} J\dot{\omega} + k_\gamma\gamma_e^+\dot{\gamma} + k_\Omega\Omega_e^+\dot{\Omega} \\ = -(\omega_t I_{ws}\Omega - k_\gamma\gamma_e^+)u_1 - (I_{ws}\omega_e - k_\Omega\Omega_e^+)u_2 \qquad (46)$$

Choosing a control law as

$$u_1 = \dot{\gamma} = k_3(\omega_t I_{ws}\Omega - k_\gamma\gamma_e^+), \qquad k_3 > 0 \qquad (47a)$$

$$u_2 = \dot{\Omega} = k_4(I_{ws}\omega_s - k_\Omega\Omega_e^+), \qquad k_4 > 0 \qquad (47b)$$

yields

$$\dot{V}_2^+ = -k_3(\omega_t I_{ws}\Omega - k_\gamma\gamma_e)^2 - k_4(I_{ws}\omega_s - k_\Omega\Omega_e^+)^2 \leq 0 \qquad (48)$$

The last inequality implies, in particular, that the angular velocity remains bounded.

Now, let us check whether there exist nontrivial equilibria that make $\dot{V}_2^+ = 0$, as we did in Sec. V.A. These equilibria are characterized by the equations

$$\omega_t I_{\mathrm{ws}} \Omega - k_\gamma \gamma_e = 0 \quad \text{and} \quad I_{\mathrm{ws}} \omega_s - k_\Omega \Omega_e^+ = 0 \qquad (49)$$

There are three types of nontrivial equilibria, and are shown in Table 1. See Appendix B for the details.

Similarly, we also consider a nonlinear controller for the negative final wheel speed Ω_f^-. Define another Lyapunov function candidate $V_2^-(\omega, \gamma_e^-, \Omega_e^-)$ as

$$\begin{aligned} V_2^-(\omega, \gamma_e^-, \Omega_e^-) &\triangleq \frac{1}{2}\omega^{\mathsf{T}} J\omega + \frac{1}{2}k_\gamma \gamma_e^{-2} + \frac{1}{2}k_\Omega \Omega_e^{-2} \\ &= \frac{1}{2}(J_t(\omega_s^2 + \omega_t^2) + J_a\omega_g^2) + \frac{1}{2}k_\gamma \gamma_e^{-2} + \frac{1}{2}k_\Omega \Omega_e^{-2} \end{aligned} \qquad (50)$$

where $\gamma_e^- \triangleq \gamma - \gamma_f^-$ and $\Omega_e^- \triangleq \Omega - \Omega_f^-$. This Lyapunov function candidate suggests the control law

$$u_1 = \dot{\gamma} = k_3(\omega_t I_{\mathrm{ws}}\Omega - k_\gamma \gamma_e^-), \qquad k_3 > 0 \qquad (51a)$$

$$u_2 = \dot{\Omega} = k_4(I_{\mathrm{ws}}\omega_s - k_\Omega \Omega_e^-), \qquad k_4 > 0 \qquad (51b)$$

One can show that the nontrivial equilibria of this control law are identical with those of the control law (47) shown in Table 1, except that ω_s and Ω have opposite sign.

Since it is rather complicated to check the stability of these nontrivial equilibria using Lyapunov's first method as we did in Sec. V.A, here we follow a different approach. We eliminate the possibility of encountering these nontrivial equilibria altogether, by properly choosing the values of the controller gains, and by utilizing the controller designed in Sec. V.A, which stabilizes the angular velocity ω. To this end, let $V_{2\mathrm{eq}}$ be the minimum of the values of the Lyapunov candidates V_2^+ and V_2^- at the nontrivial equilibria. That is, let

$$V_{2\mathrm{eq}} \triangleq \min\left\{ \frac{1}{2}H_0^2\left(\frac{1}{J_t} + \frac{k_\Omega}{I_{\mathrm{ws}}^2}\right), \right.$$
$$\left. \frac{2k_\Omega H_0^2}{I_{\mathrm{ws}}^2 + k_\Omega J_t}, \frac{1}{2}\frac{H_0^2(I_{\mathrm{ws}}^2 + k_\Omega J_t)}{J_a(k_\Omega(J_t - J_a) + I_{\mathrm{ws}}^2)} \right\} > 0 \qquad (52)$$

For any nonzero initial angular momentum $\boldsymbol{H}_0$ and any spacecraft inertia matrix J, we can choose the control gains k_γ and k_Ω so that

$$V_{2\mathrm{eq}} > \frac{1}{2}k_\gamma \pi^2 \qquad (53)$$

If we take the value of the gimbal angle γ using the "congruence"-function modulo 2π, that is,

$$\begin{aligned} \gamma^+ &= \mathrm{mod}(\gamma + \pi - \gamma_f^+, 2\pi) - \pi + \gamma_f^+ \\ \gamma^- &= \mathrm{mod}(\gamma + \pi - \gamma_f^-, 2\pi) - \pi + \gamma_f^- \end{aligned} \qquad (54)$$

and redefine

$$\gamma_e^+ \triangleq \gamma^+ - \gamma_f^+, \qquad \gamma_e^- \triangleq \gamma^- - \gamma_f^- \qquad (55)$$

then the gimbal angle errors are confined as $-\pi \leq \gamma_e^+ < \pi$ and $-\pi \leq \gamma_e^- < \pi$.

Now, suppose that the control law (37) is applied to make $\omega \to 0$. From momentum conservation, the wheel speed Ω converges to either Ω_f^+ or Ω_f^-, as $\omega \to 0$. If we let $\epsilon \triangleq V_{2\mathrm{eq}} - \frac{1}{2}k_\gamma \pi^2 > 0$ from Eq. (53), then there exist a time $t_s > 0$ such that

$$\frac{1}{2}(\omega^{\mathsf{T}} J\omega + k_\Omega \Omega_e^{+2})|_{t=t_s} < \epsilon, \quad \text{or} \quad \frac{1}{2}(\omega^{\mathsf{T}} J\omega + k_\Omega \Omega_e^{-2})|_{t=t_s} < \epsilon \qquad (56)$$

At this time t_s, therefore, one of the following conditions must hold

$$V_2^+(t = t_s) < \epsilon + \frac{1}{2}k_\gamma \gamma_e^{+2} < \epsilon + \frac{1}{2}k_\gamma \pi^2 = V_{2\mathrm{eq}} \qquad (57a)$$

$$V_2^-(t = t) < \epsilon + \frac{1}{2}k_\gamma \gamma_e^{-2} < \epsilon + \frac{1}{2}k_\gamma \pi^2 = V_{2\mathrm{eq}} \qquad (57b)$$

Hence, if we switch the controller at $t = t_s$ from Eq. (37) to Eqs. (47) or (51), depending on the sign of the wheel speed Ω, then we ensure that $\gamma \to \gamma_f^+$ and $\Omega \to \Omega_f^+$, or $\gamma \to \gamma_f^-$ and $\Omega \to \Omega_f^-$ as $\omega \to 0$, respectively, without encountering any of the nontrivial equilibria. This follows from the fact that the control laws (47) and (51) imply $\dot{V}_2^+ \leq 0$ and $\dot{V}_2^- \leq 0$, respectively.

Remark 1: Inequality (53) imposes a restriction on the controller gain k_γ that depends on the initial conditions for H_0, equivalently $\| \omega(0) \|$. For every bounded set of initial conditions the controller gain can be chosen such that this inequality is satisfied. This type of stability is known in the literature as semiglobal stability.

Remark 2: Notice that, assuming $2J_a - J_t > 0$ holds, then condition (53) can be satisfied by choosing $k_\Omega > 0$ and $k_\gamma > 0$ as follows

$$k_\Omega > \frac{I_{\mathrm{ws}}^2}{\min\{J_t, 2J_a - J_t\}} \quad \text{and} \quad \frac{2k_\Omega H_0^2}{I_{\mathrm{ws}}^2 + k_\Omega J_t} > \frac{1}{2}k_\gamma \pi^2 \qquad (58)$$

See also the discussion in Appendix B.

C. Nonlinear Control Design for Stabilization of ω, γ_e, and ϕ_e

The final goal of the control design is to stabilize ϕ_e, as well as ω and γ_e. We already have designed three separate controllers, which we will use in the sequel to fulfill this objective. One is a linear controller, designed in Sec. IV, which locally stabilizes ω, γ_e, and ϕ_e. The second one is a nonlinear controller, designed in Sec. V.A, which regionally stabilizes ω. The third one designed in Sec. V.B makes $\omega \to 0$, as well as $\gamma \to \gamma_f$ and $\Omega \to \Omega_f$. Each one of the first and the third controllers has two different versions according to the sign of Ω_f. Utilizing these three control laws, we can construct a switching control logic consisting of three control phases that regionally achieves the final control objective given in Eq. (17). At the first stage, we use the nonlinear controller (37) to make $\omega \to 0$. While this controller is being applied, the values of V_2^+ and V_2^- are monitored, and if one of them becomes less than $V_{2\mathrm{eq}}$, then the control switches to the second stage, where the controller (47) or (51) results in $\omega \to 0$ and $\gamma \to \gamma_f^\pm$ and $\Omega \to \Omega_f^\mp$ according to the sign of Ω_f. At the third stage, we use the linear controller in Sec. IV to also stabilize ϕ_e as well as ω and γ_e.

To use the linear controller in the third stage, we need all the states to be kept close to their desired equilibrium values, except ϕ_e which

Table 1 Nontrivial equilibria of the system under controller Eq. (47)

Type	E1[a]	E2	E3[b]
ω_s	$-(k_\Omega H_0/I_{\mathrm{ws}}^2)$	$-[2H_0/(J_t + I_{\mathrm{ws}}^2/k_\Omega)]$	$H_0/(J_a - J_t - I_{\mathrm{ws}}^2/k_\Omega)$
ω_t	$\pm\sqrt{[H_0^2/I_{\mathrm{ws}}^4][(I_{\mathrm{ws}}^4/J_t^2) - k_\Omega^2]}$	0	0
ω_g	0	0	$\pm\sqrt{H_0^2\{(1/J_a^2) - [1/(J_a - J_t - I_{\mathrm{ws}}^2/k_\Omega)^2]\}}$
γ_e^+	0	0	0
Ω	0	$[-2I_{\mathrm{ws}}H_0/(J_t k_\Omega + I_{\mathrm{ws}}^2)] + (H_0/I_{\mathrm{ws}})$	$-\{I_{\mathrm{ws}}H_0/[k_\Omega(J_t - J_a) + I_{\mathrm{ws}}^2]\} + (H_0/I_{\mathrm{ws}})$
V_2^+	$\frac{1}{2}H_0^2[(1/J_t) + (k_\Omega/I_{\mathrm{ws}}^2)]$	$2k_\Omega H_0^2/(I_{\mathrm{ws}}^2 + k_\Omega J_t)$	$(1/2)\{[H_0^2(I_{\mathrm{ws}}^2 + k_\Omega J_t)]/\{J_a[k_\Omega(J_t - J_a) + I_{\mathrm{ws}}^2]\}\}$

[a]Exists only if $k_\Omega \leq I_{\mathrm{ws}}^2/J_t$.
[b]Exists only if $2J_a - J_t - I_{\mathrm{ws}}^2/k_\Omega \leq 0$.

is ignorable, that is, it has no effect on the differential equations. It follows that $\omega \approx 0$, $\gamma_e \approx 0$, $\Omega \approx \Omega_f^{\pm}$ at the beginning of, and during the third stage. Owing to the nonlinear controller used at the second stage ω and γ_e have arbitrarily small values at the beginning of the third stage. The wheel speed Ω also becomes $\Omega = \Omega_f^{\pm}$ to conserve the total angular momentum. In addition, if we determine the weighting matrix Q and R in the performance index (32) so that the weights on ω and γ_e are large, then the LQR controller that minimizes the performance index in (32) will keep ω and γ_e small during the third stage. The wheel speed variation also must be kept small, that is, $\Omega \approx \Omega_f^{\pm}$, but this is not guaranteed by the LQR controller. From the momentum conservation law, however, if we can keep ω sufficiently small during the third stage (by using a large weight on ω in the LQR controller), then Ω will also stay close to $\Omega_f^{\pm}$. The flow chart of Fig. 6 summarizes the whole procedure to achieve the control objective.

D. A Comparison with the Momentum-Bias Case

Passive partial control of a satellite using a single (nongimballed) wheel is a widely used and very well understood technique in practice. See [[29], Chap. 6] and [[30], Chap. 8]. A momentum-biased satellite, for instance, uses a single wheel to provide gyroscopic stability of the wheel body-fixed axis. The body-fixed axis along the wheel spin axis thus remains stable (but not asymptotically stable). The projection of the angular velocity vector along the transverse axes is not zero, however, and this induces nutation of the body-fixed wheel axis at a frequency approximately equal to [29,30]

$$\omega_{\text{nut}} = \frac{\Omega I_{\text{ws}}}{\sqrt{J_a J_t}} \tag{59}$$

In this section we investigate the relationship of this classical result to the stabilizing control law of Sec. V.A, and we elucidate the effect of using an active control strategy to inject damping in to the system in order to make it asymptotically (not merely Lyapunov) stable.

To this end, we linearize the closed-loop dynamics (A1) around the desired equilibrium
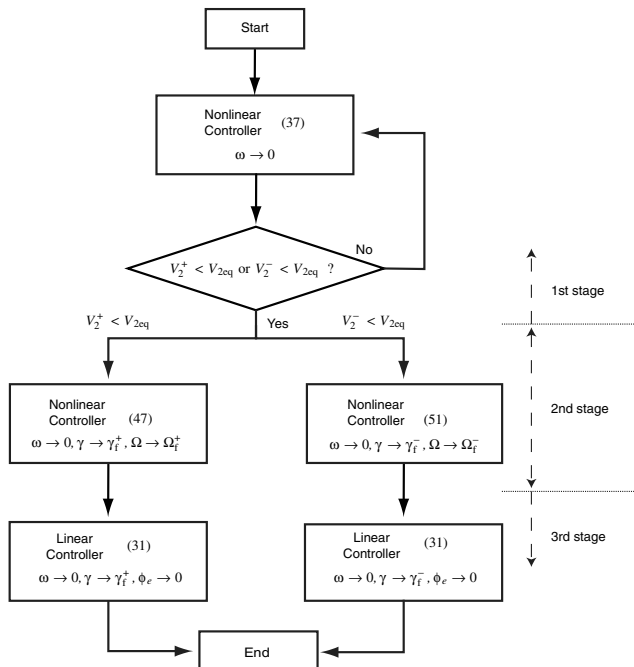
$$\omega = 0, \qquad \Omega \neq 0$$

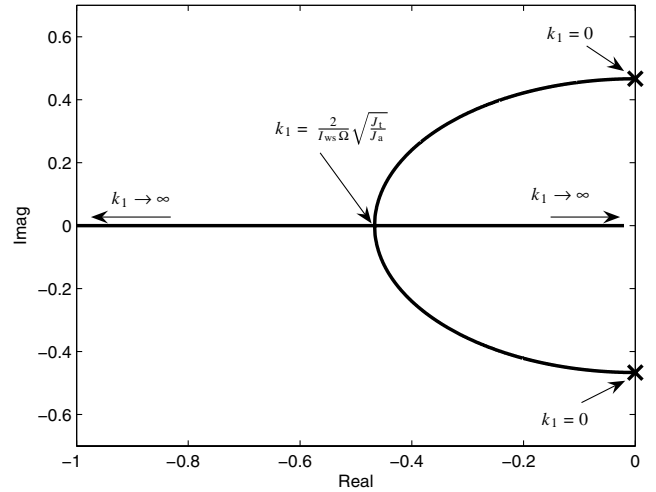Fig. 6 Flow chart of entire control procedure.

Fig. 7 Locus of closed-loop eigenvalues for $0 \leq k_1 < \infty$.

The linearized equations are given by

$$J\Delta\dot{\omega} = [(I_{\text{ws}}\Omega\hat{s})^{\times} - k_2 I_{\text{ws}}^2 \hat{s}\hat{s}^{\mathsf{T}} - k_1 I_{\text{ws}}^2 \Omega^2 \hat{t}\hat{t}^{\mathsf{T}}]\Delta\omega$$

which, when expressed in the stationary gimbal frame ($\Delta\dot{\gamma} = 0$), leads to a linear system with state matrix

$$\begin{bmatrix} -k_2 I_{\text{ws}}^2/J_t & 0 & 0 \\ 0 & -k_1 I_{\text{ws}}^2\Omega^2/J_t & -I_{\text{ws}}\Omega/J_t \\ 0 & I_{\text{ws}}\Omega/J_a & 0 \end{bmatrix}$$

This matrix has eigenvalues

$$-\frac{k_2 I_{\text{ws}}^2}{J_t}, \qquad \frac{\Omega I_{\text{ws}}}{2 J_t J_a}\left(-J_a k_1 I_{\text{ws}}\Omega \pm \sqrt{J_a^2 k_1^2 I_{\text{ws}}^2 \Omega^2 - 4 J_t J_a}\right) \tag{60}$$

Since all three eigenvalues are in the open left half of the complex plane for all positive values of k_1 and k_2, *asymptotic* stability results, as expected. In the absence of feedback ($k_1 = k_2 = 0$) we have the standard case of a gyrostat [[29], p. 162] and the system has a pair of purely imaginary eigenvalues at

$$\pm i \frac{\Omega I_{\text{ws}}}{\sqrt{J_a J_t}}$$

that signify a nutation frequency as in (59). Note that the effect of the feedback control action is to add damping to the system and move eigenvalues further into the open left half of the complex plane, at least initially. From (60) it is evident that for large values of k_1 all three roots are on the real axis and the response can be made nonoscillatory. This will occur for

$$k_1 > k_{1\text{crit}} = \frac{2}{I_{\text{ws}}\Omega}\sqrt{\frac{J_t}{J_a}}$$

which is the optimal choice of k_1 for a fast response. Figure 7 shows a typical root locus for the closed-loop system eigenvalues as a function of the controller gain k_1. In Fig. 7 only two of the roots are shown as the third one depends solely on k_2 and remains always negative real for all $k_2 > 0$.

VI. Numerical Examples

In this section, we give an illustrative example of the proposed control design for the problem of spacecraft angular velocity stabilization with simultaneous body-fixed line-of-sight control. In the previous sections, the simplified equations of motion with the assumptions $\dot{J} = 0$ and $I_{\text{cg}}\ddot{\gamma}\hat{g} = 0$ were used for control design. In this section the complete nonlinear equations of motion given by

Table 2   Spacecraft model parameters

Symbol	Value	Units
$^B I$	$\begin{bmatrix} 20 & 0 & 0 \\ 0 & 20 & 0 \\ 0 & 0 & 10 \end{bmatrix}$	kg m^2
I_{ws}	0.0042	kg m^2
I_{wt}, I_{wg}	0.0024	kg m^2
I_{gs}	0.0093	kg m^2
I_{gt}, I_{gg}	0.0054	kg m^2
$\hat{s}_0$	$[1, 0, 0]^\mathsf{T}$	——
$\hat{t}_0$	$[0, 1, 0]^\mathsf{T}$	——
$\hat{g}_0$	$[0, 0, 1]^\mathsf{T}$	——

Table 3   Control design parameters and initial conditions

Symbol	Value	Units
$q(0)$	$[0, 0, 0, 1]^\mathsf{T}$	——
$\omega(0)^a$	$[0.2, -0.4, 0.1]^\mathsf{T}$	rad/ sec
$\gamma(0)$	120	deg
$\dot{\gamma}(0)$	0	deg / sec
$\Omega(0)$	3×10^3	rpm
$\hat{n}^b$	$(1/\sqrt{5})[1, 2, 0]^\mathsf{T}$	——
Q	diag$[10^4, 10^4, 10^4, 10^3, 10^3]$	——
R	diag$[10^3, 1]$	——
k_1, k_3	1	——
k_2, k_4	5×10^4	——
k_γ	0.05	——
k_Ω	1×10^{-6}	——
K_p	1	——

^{a}Written in the body frame $\mathcal{B}$.
^{b}Written in the inertial frame $\mathcal{I}$.

Eq. (1) and the acceleration steering law of [22,24] are used to predict and validate the performance of the proposed controllers under realistic conditions. Table 2 summarizes the values of the moments of inertia of the spacecraft and the VSCMG used in all numerical simulations.

The control design parameters, the initial conditions, and the desired line of sight $\hat{n}$ used in the simulations are given in Table 3. To describe the attitude of the spacecraft with respect to the inertial frame $\mathcal{I}$, we use Euler's parameters (quaternion). The attitude of the spacecraft with respect to the $\mathcal{H}$ frame is described by means of the 3-1-3 Eulerian angles ϕ, θ, and ψ as described earlier. The initial value of the quaternion vector in Table 3 implies that the initial body
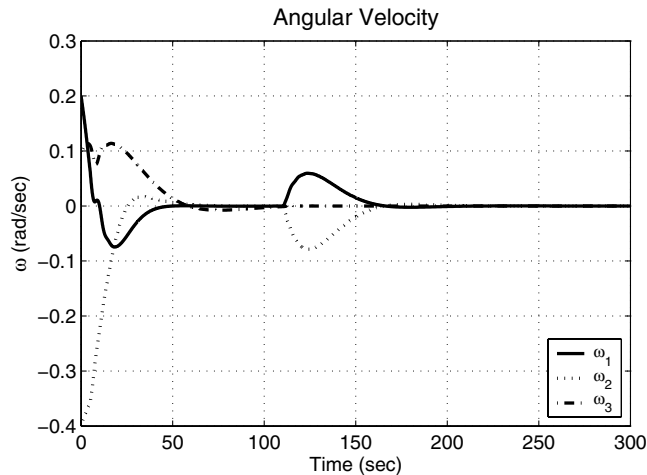
Fig. 8   Spacecraft angular velocity history $\omega(t)$.

Lyapunov Function V_2^-
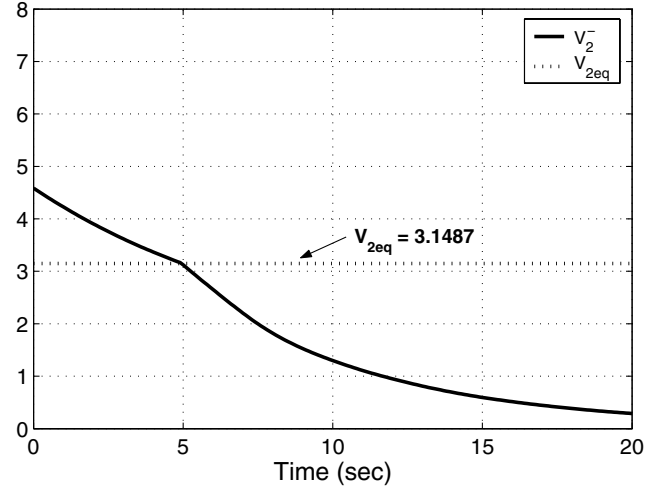
Fig. 9   Lyapunov function candidate history $V_2^-(t)$.

frame $\mathcal{B}$ is aligned with the inertial frame $\mathcal{I}$ at $t = 0$. The controller gains of the nonlinear controller and the weights of the LQR controller are chosen by trial and error in order to stabilize the system quickly and with suitable damping. In particular, the gains k_γ and k_Ω are chosen so that the condition (53) holds.

For the given initial angular velocity $\omega(0)$ and the desired line-of-sight direction vector $\hat{n}$, the corresponding final gimbal angles are calculated from Eq. (16) as $\gamma_f^+ = 127.1°$ and $\gamma_f^- = -52.91°$. The final wheel speeds are given by $\Omega_f^+ = H_0/I_{ws} = 17,505$ rpm and $\Omega_f^- = -H_0/I_{ws} = -17,505$ rpm. In addition, the inertial frame $\mathcal{H}$, defined from (7) and (8), is given via

$$R_{\mathcal{I}}^{\mathcal{H}} = \begin{bmatrix} \hat{a}_1^\mathsf{T} \\ \hat{a}_2^\mathsf{T} \\ \hat{a}_3^\mathsf{T} \end{bmatrix} = \begin{bmatrix} 0.8889 & 0.4474 & 0.0983 \\ -0.1458 & 0.0729 & 0.9866 \\ 0.4342 & -0.8914 & 0.1300 \end{bmatrix} \quad (61)$$

Using this matrix we can calculate the coordinates of $\hat{n}$ in the $\mathcal{H}$ frame as $\hat{n} = [0.7977, 0, -0.6031]^\mathsf{T}$.

Figures 8–13 show the results of the numerical simulations. As mentioned in Sec. V.C, the whole control procedure consists of three stages. During the first stage, the nonlinear controller (37) is applied so as to stabilize ω, whereas γ and ϕ are allowed to take any values. For this example, V_2^- becomes less than $V_{2eq} = 3.1487$ at $t_{s1} \approx 4.98$ sec, as shown in Fig. 9, so that the control mode is switched to the second stage of the nonlinear controller (51). During the second stage, ω is still under stabilization, and $\gamma \to \gamma_f^-$ and $\Omega \to \Omega_f^-$.

The switching from the second stage to the third stage occurs when the norms of ω and γ_e become smaller than some given tolerances $\epsilon_\omega, \epsilon_\gamma > 0$, respectively. We have used $\epsilon_\omega = 10^{-3}$ and $\epsilon_\gamma = 10^{-2}$ in the simulations, and the switching time for these values was $t_{s2} \approx 110.66$ sec. At the third stage, the linear LQR controller is applied to achieve the overall control objective by making ω, γ_e, and ϕ_e all converge to zero.

Figure 8 shows the angular velocity trajectory of the spacecraft. As expected, the angular velocity is reduced to zero, then momentarily it diverges after switching from the second to the third stage (near $t_{s2} = 110.66$ s), and it converges to zero again as $t \to \infty$. Notice that $\omega_3 = \omega_g$ is kept small even during the third stage. This means that the spacecraft does not rotate significantly about the gimbal axis, but it does rotate about the spin axis in order to make $\phi_e \to 0$. On the other hand, the other two angular velocity elements noticeably increase during the transition to the third stage. This increase can be mitigated by a suitable choice of the matrices Q and R in Eq. (32).

Figure 10 shows the attitude history of the body frame $\mathcal{B}$. Figure 10a is the time history of the quaternion parameters of $\mathcal{B}$ with
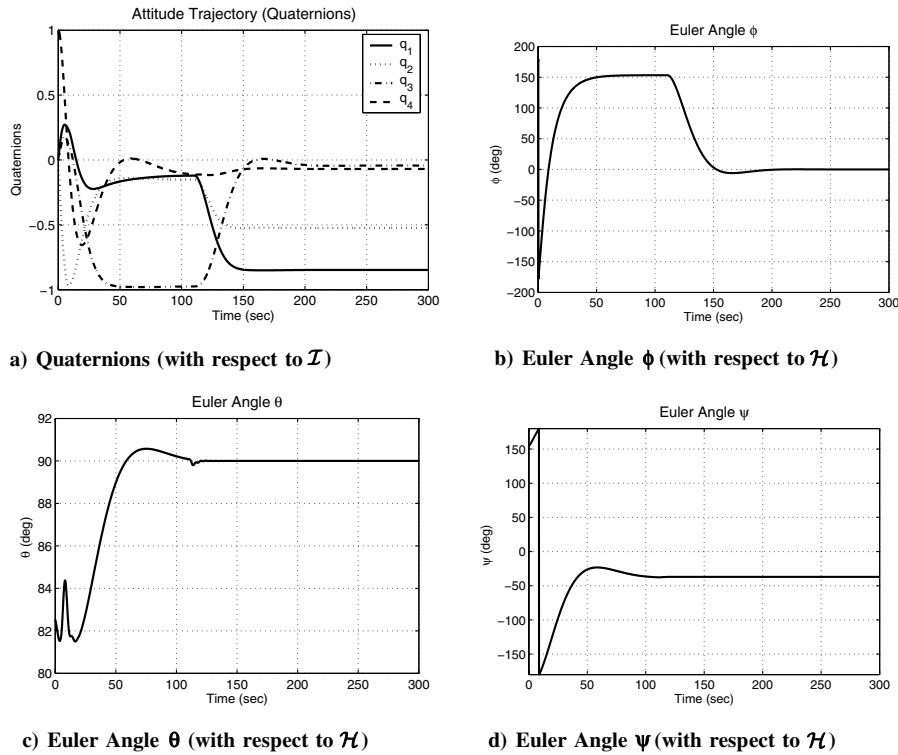
a) Quaternions (with respect to $\mathcal{I}$)

b) Euler Angle ϕ (with respect to $\mathcal{H}$)

c) Euler Angle θ (with respect to $\mathcal{H}$)

d) Euler Angle ψ (with respect to $\mathcal{H}$)

Fig. 10   Spacecraft attitude trajectories.
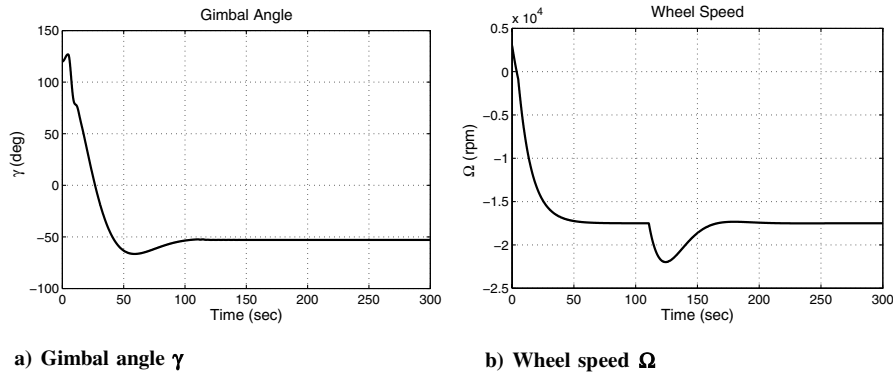

a) Gimbal angle γ

b) Wheel speed Ω

Fig. 11   Gimbal angle and wheel speed.

respect to $\mathcal{I}$. Before the switching from the second to the third stage, the attitude parameters converge to certain constant values because $\omega \to 0$, due to the nonlinear controller, and after switching they converge to some other values as $\omega \to 0$ again, due to the linear LQR controller. The final quaternion coincides with the desired final quaternion vector. Specifically, we may check that the final $\hat{\boldsymbol{b}}_1$ axis is

$$\hat{\boldsymbol{b}}_1 = [0.4472, 0.8944, 0]^{\mathsf{T}} \approx \hat{\boldsymbol{n}}$$

which means that the line of sight fixed along the $\hat{\boldsymbol{b}}_1$ axis points in the given direction $\hat{\boldsymbol{n}}$, as desired.

Figures 10b–10d show the time history of the Eulerian angles of $\mathcal{B}$ with respect to $\mathcal{H}$, which are used for the parametrization of the spacecraft orientation at rest. As the angular velocity converges to zero, θ converges to $\theta_f = 90$ deg as expected. As shown in Fig. 10b, ϕ is not controlled during the first and second stage, but after switching to the third stage, ϕ converges to zero via the use of the LQR controller. The other Euler angle ψ also converges to $\psi_f = \tan^{-1}(n_3/n_1) = \tan^{-1}(-0.6031/0.7977) = -37.09$ deg. We can see that only ϕ varies in the third stage, whereas θ and ψ are

nearly kept constant, and this implies again that the spacecraft rotates about the VSCMG wheel spin axis during the third stage.

Figure 11 shows the gimbal angle and the wheel speed trajectories of the VSCMG, respectively. It can be shown that both the gimbal angle changes and the wheel speed changes are exploited by the controller during the first and second stages to stabilize ω and γ_e. In the third stage, only the wheel speed change is exploited to make $\phi \to 0$. The variation of the wheel speed in the third stage is not very large, so that the use of the linearized analysis is justified. In fact, we can make the difference $\Omega - \Omega_f$ much smaller by weighting less ϕ or weighting more ω and/or $\dot{\Omega}$ in the performance index (32), but the convergence rate of ϕ will become slower in this case. It is also shown that the gimbal angle γ converges to $\gamma_f^- = -52.91$ deg, which satisfies Eq. (11). Figure 12 shows the trajectories of the control inputs, $\dot{\gamma}$ and $\dot{\Omega}$, as well the gimbal acceleration $\ddot{\gamma}$.

Finally, Fig. 13 shows a series of snapshots of the whole maneuver of the spacecraft. Note that the total angular momentum vector $\boldsymbol{H}$ is fixed in inertial space during the maneuver. The angular velocity ω is gradually reduced to zero and it is hardly seen in these snapshots after $t = 40$ sec. At $t = 100$ sec, which is just before the switching from

a) Gimbal rate $\dot{\gamma}$

b) Gimbal acceleration $\ddot{\gamma}$

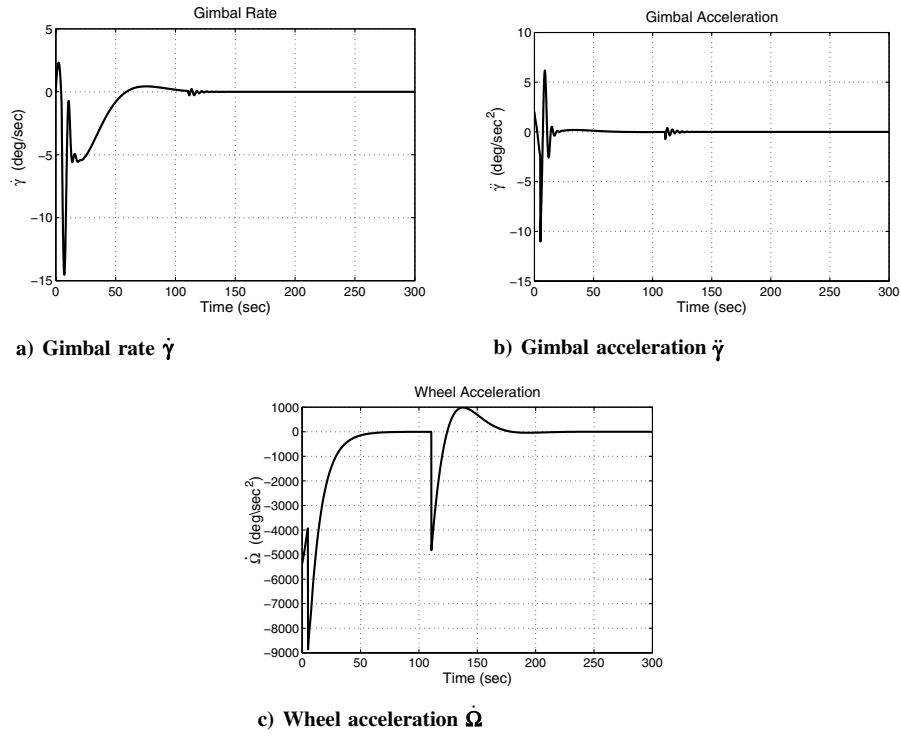c) Wheel acceleration $\dot{\Omega}$

Fig. 12   Control inputs.

the second to the third stage, the gimbal angle is $\gamma_f^- = -52.91$ deg. Notice the relative positions of the unit vectors $\hat{\boldsymbol{b}}_1$ and $\hat{\boldsymbol{s}}$ about the $\hat{\boldsymbol{b}}_3$ axis. The spin axis $\hat{\boldsymbol{s}}$ is perfectly opposite in direction to $\boldsymbol{H}$, and the wheel speed is $\Omega = \Omega_f^- < 0$, which means that the wheel is actually spinning in the direction of $\boldsymbol{H}$ to conserve the angular momentum. At

$t = 120$ sec, which is just after the second switching, we may see that the spacecraft rotates about the $\hat{\boldsymbol{s}}$ axis to align the $\hat{\boldsymbol{b}}_1$ axis with $\hat{\boldsymbol{n}}$, while controlled by the LQR controller. Near $t = 200$ sec., the spacecraft is at rest with the $\hat{\boldsymbol{b}}_1$ axis pointing in the direction of $\hat{\boldsymbol{n}}$, and the control objective is successfully achieved.

a) $t = 0$ sec

b) $t = 20$ sec

c) $t = 40$ sec

d) $t = 60$ sec

e) $t = 80$ sec

f) $t = 100$ sec

g) $t = 120$ sec

h) $t = 140$ sec

i) $t = 160$ sec

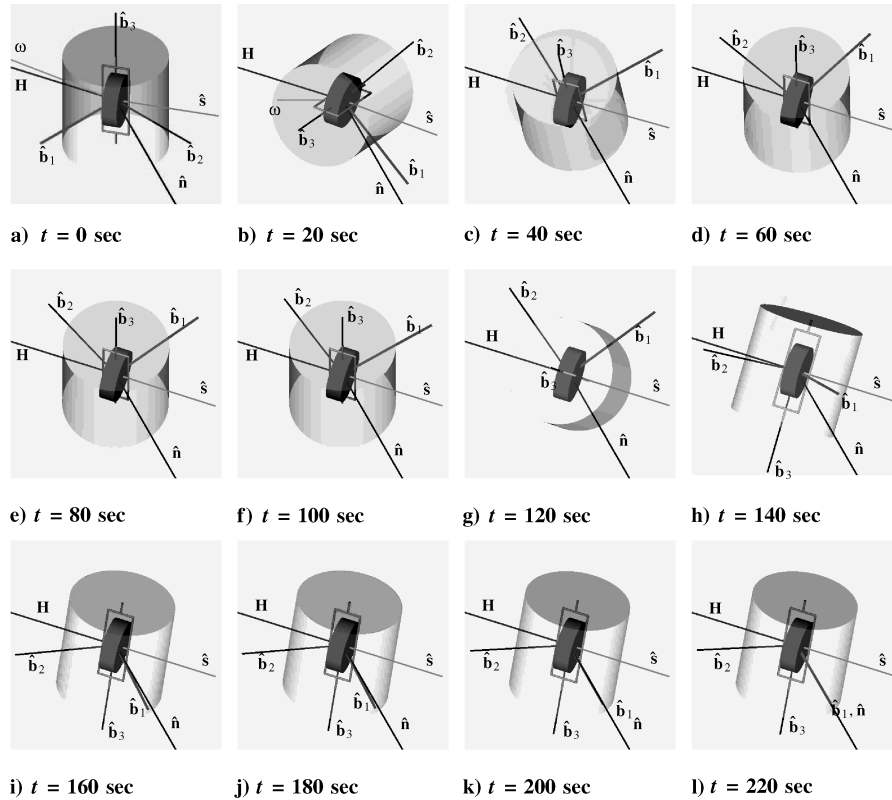j) $t = 180$ sec

k) $t = 200$ sec

l) $t = 220$ sec

Fig. 13   Snapshots of the spacecraft orientation during the maneuver.

VII. Conclusions

The present paper deals with the attitude control problem of a rigid spacecraft using only one VSCMG. It is shown that the complete attitude equations are not controllable, but a certain type of partial attitude control without violating the angular momentum conservation principle is possible. As an example of partial attitude control, the problem of controlling an axis fixed in the spacecraft frame is addressed. The approach is based on the complete characterization of all feasible final orientations of the spacecraft at rest by a pair of two angles. Both linear (for small initial conditions) and nonlinear (for large initial conditions) strategies are presented. The proposed nonlinear control strategy consists of three consecutive stages and it successfully stabilizes the spacecraft angular velocity at large, while making a specified spacecraft body-fixed axis aim at a given inertial direction. The results of this paper should be useful for spacecraft missions where only two-axis stabilization is of interest (e.g., the line-of-sight direction of a camera or antenna) or for mitigating actuator failures. This paper is the first one dealing with the problem of spacecraft attitude stabilization using a single VSCMG. Several extensions are therefore possible. Future work should deal with the general case of a nonaxisymmetric spacecraft and/or with the case of zero total initial angular momentum, as well as robustness issues.

Appendix A: Instability of the Nontrivial Equilibria

In this Appendix, we show that the nontrivial equilibrium states of Eqs. (3) and (37) are unstable. For simplicity of the ensuing analysis, we assume that $h \triangleq J\omega + I_{cg}\dot{\gamma}\hat{g} + I_{ws}\Omega\hat{s} \approx J\omega + I_{ws}\Omega\hat{s}$, which is justified by the fact that the gimbal angle rate $\dot{\gamma}$ does not contribute significantly to the total angular momentum. The closed-loop system with the proposed nonlinear controller (37) can be written as

$$J\dot{\omega} = -\omega^\times(J\omega + I_{ws}\Omega\hat{s}) - k_1 I_{ws}^2 \Omega^2 \omega_t \hat{t} - k_2 I_{ws}^2 \omega_s \hat{s} \quad \text{(A1)}$$

$$\dot{\gamma} = k_1 I_{ws}\Omega\omega_t \quad \text{(A2)}$$

$$\dot{\Omega} = k_2 I_{ws}\omega_s \quad \text{(A3)}$$

Linearizing these equations about $\Omega = 0$, $\gamma_e = 0$, $\omega_t = 0$, and $\omega_g = \pm H_0/J_a$, one obtains

$$J\Delta\dot{\omega} = [(J\omega)^\times - \omega^\times J - k_2 I_{ws}^2 \hat{s}\hat{s}^\mathsf{T}]\Delta\omega - \omega^\times I_{ws}\hat{s}\Delta\Omega \quad \text{(A4)}$$

$$\Delta\dot{\gamma} = 0 \quad \text{(A5)}$$

$$\Delta\dot{\Omega} = k_2 I_{ws}\hat{s}^\mathsf{T}\Delta\omega \quad \text{(A6)}$$

It is obvious that the dynamics of $\Delta\gamma$ in Eq. (A5) is neutrally stable, and can be decoupled from those of $\Delta\omega$ and $\Delta\Omega$. Thus we only need to check the stability of Eqs. (A4) and (A6). It can be easily shown that the characteristic equation of this linear system is

$$\lambda(\lambda^3 + a_2\lambda^2 + a_1\lambda + a_0) = 0 \quad \text{(A7)}$$

where

$$a_2 = (1/J_t)k_2 I_{ws}^2,$$
$$a_1 = \frac{H_0^2(J_a - J_t)^2}{J_t^2 J_a^2},$$
$$a_0 = -\frac{I_{ws}^2 k_2 H_0^2 (J_a - J_t)}{J_t^2 J_a^2}$$

This equation has a single root at the origin, so that the system is marginally stable at best. From Routh's stability criterion, a necessary and sufficient condition for stability for the characteristic equation (A7) is

$$a_0 > 0, \qquad a_1 > 0, \qquad a_2 > 0$$

and

$$a_2 a_1 - a_0 = \frac{I_{ws}^2 k_2 H_0^2 (J_a - J_t)}{J_a J_t^3} > 0$$

Note, however, that a_0 and $(a_2 a_1 - a_0)$ cannot have a same sign. Therefore, this equilibrium is unstable.

Similarly, consider the equilibrium $\Omega = 0$, $\gamma_e = 0$, $\omega_g = 0$, and $\omega_t = \pm H_0/J_t$. The linearized equations about this equilibrium state are

$$J\Delta\dot{\omega} = [(J\omega)^\times - \omega^\times J - k_2 I_{ws}^2 \hat{s}\hat{s}^\mathsf{T}]\Delta\omega \\ - k_2 I_{ws}^2 \omega_t \hat{s}\Delta\gamma - \omega^\times I_{ws}\hat{s}\Delta\Omega \quad \text{(A8)}$$

$$\Delta\dot{\gamma} = k_1 \omega_t I_{ws}\Delta\Omega \quad \text{(A9)}$$

$$\Delta\dot{\Omega} = k_2 I_{ws}\hat{s}^\mathsf{T}\Delta\omega + k_2 \omega_t I_{ws}\Delta\gamma \quad \text{(A10)}$$

The characteristic equation of this linear system is

$$\lambda^2(\lambda^3 + a_2\lambda^2 + a_1\lambda + a_0) = 0 \quad \text{(A11)}$$

where

$$a_2 = (1/J_t)k_2 I_{ws}^2, \qquad a_1 = -\frac{k_1 I_{ws}^2 k_2 H_0^2}{J_t^2}$$
$$a_0 = \frac{I_{ws}^2 k_2 H_0^2}{J_t^3 J_a}(J_a - J_t)$$

One of the necessary conditions for stability is

$$a_1 > 0$$

which is false for this system, because $k_1, k_2 > 0$ from (37). Therefore, this equilibrium is also unstable, and the proof is complete.

Appendix B: Characterization on the Nontrivial Equilibria

In this Appendix we derive the nontrivial equilibrium states of the closed-loop system under the nonlinear controller (47). These equilibria are characterized by Eq. (49), which is rewritten here as

$$\omega_t I_{ws}\Omega - k_\gamma \gamma_e = 0 \quad \text{and} \quad I_{ws}\omega_s - k_\Omega \Omega_e^+ = 0 \quad \text{(B1)}$$

We consider two cases: 1) $\Omega = 0$ and 2) $\Omega \neq 0$.

1) $\Omega = 0$: When $\Omega = 0$, then $\Omega_e^+ = -\Omega_f^+ = -H_0/I_{ws}$, and thus $\omega_s = -k_\Omega H_0/I_{ws}^2$ is a nonzero constant. Rewriting the dynamic equations in the gimbal frame $\mathcal{G}$, one obtains $J\dot{\omega} = -\omega^\times J\omega$, where $\omega = [\omega_s, \omega_t, \omega_g]^\mathsf{T}$, $\dot{\omega} = [0, \dot{\omega}_t, \dot{\omega}_g]^\mathsf{T}$. This equation can be written componentwise as

$$\begin{bmatrix} 0 \\ J_t\dot{\omega}_t \\ J_a\dot{\omega}_g \end{bmatrix} = \begin{bmatrix} (J_t - J_a)\omega_t\omega_g \\ -(J_t - J_a)\omega_g\omega_s \\ 0 \end{bmatrix} \quad \text{(B2)}$$

which immediately yields $\omega_t\omega_g = 0$ and $\dot{\omega}_g = 0$. Moreover, because ω_s and ω_g are constant, $\dot{\omega}_t$ is constant, from the second element of Eq. (B2). If $\dot{\omega}_t$ is a nonzero constant, ω_t will diverge to infinity thus violating the boundedness of ω. Thus, $\dot{\omega}_t = 0$ and $\omega_g\omega_s = 0$. Since $\omega_s = -k_\Omega H_0/I_{ws}^2 \neq 0$, it follows that $\omega_g = 0$. Therefore, the total angular momentum is

$$h = \left[-J_t \frac{k_\Omega H_0}{I_{ws}^2}, J_t\omega_t, 0 \right]^\mathsf{T} \quad \text{(B3)}$$

Thus, assuming that $k_\Omega \leq I_{ws}^2/J_t$ and from $\| \boldsymbol{h} \| = H_0$, we have that

$$\omega_t = \pm \sqrt{\frac{H_0^2}{I_{ws}^4}\left(\frac{I_{ws}^4}{J_t^2} - k_\Omega^2\right)} \qquad (B4)$$

This is the nontrivial equilibrium E1 in Table 1. If, on the other hand, $k_\Omega > I_{ws}^2/J_t$, this equilibrium does not exist.

2) $\Omega \neq 0$: In this case, ω_t as well as ω_s are constant. The equation of motion written in the gimbal frame is

$$J\dot{\omega} = -\omega^\times(J\omega + I_{ws}\Omega\hat{s}) = -\omega^\times \boldsymbol{h} \qquad (B5)$$

where

$$\boldsymbol{h} = [J_t\omega_s + I_{ws}\Omega, J_t\omega_t, J_a\omega_g]^\mathsf{T} \qquad (B6)$$

and $\omega = [\omega_s, \omega_t, \omega_g]^\mathsf{T}$, $\dot{\omega} = [0, 0, \dot{\omega}_g]^\mathsf{T}$. Equivalently,

$$\begin{bmatrix} 0 \\ 0 \\ J_a\dot{\omega}_g \end{bmatrix} = \begin{bmatrix} \omega_t\omega_g(J_t - J_a) \\ \omega_g\omega_s(J_a - J_t) - I_{ws}\Omega\omega_g \\ I_{ws}\Omega\omega_t \end{bmatrix} \qquad (B7)$$

and thus $\omega_t\omega_g = 0$. Let us consider two cases again: a) $\omega_g = 0$ and b) $\omega_t = 0$.

2a) $\omega_g = 0$: Because $\dot{\omega}_g = 0$, $\omega_t = 0$ and

$$\boldsymbol{h} = [J_t\omega_s + I_{ws}\Omega, 0, 0]^\mathsf{T} = [\pm H_0, 0, 0]^\mathsf{T} \qquad (B8)$$

From Eq. (B1), $\Omega_e^+ = I_{ws}\omega_s/k_\Omega$, and thus $\Omega = \Omega_e^+ + \Omega_f^+ = I_{ws}\omega_s/k_\Omega + H_0/I_{ws}$. Comparing with the first element of (B8) yields

$$\omega_s\left(J_t + \frac{I_{ws}^2}{k_\Omega}\right) = 0, \quad \text{or} \quad \omega_s\left(J_t + \frac{I_{ws}^2}{k_\Omega}\right) = -2H_0 \qquad (B9)$$

If $\omega_s = 0$, we are done because this is the desired (trivial) equilibrium. If $\omega_s \neq 0$, then

$$\omega_s = -\frac{2H_0}{J_t + I_{ws}^2/k_\Omega} \qquad (B10)$$

and

$$\Omega = -\frac{2I_{ws}H_0}{J_t k_\Omega + I_{ws}^2} + \frac{H_0}{I_{ws}} \qquad (B11)$$

and this state corresponds to the nontrivial equilibrium E2 in Table 1.

2b) $\omega_t = 0$: From Eq. (B7), $\dot{\omega}_g = 0$, thus,

$$\omega^\times \boldsymbol{h} = 0 \qquad (B12)$$

where

$$\omega = [\omega_s, 0, \omega_g]^\mathsf{T}, \qquad \boldsymbol{h} = [J_t\omega_s + I_{ws}\Omega, 0, J_a\omega_g]^\mathsf{T} \qquad (B13)$$

Since $\boldsymbol{h} \neq 0$, this equation implies $\omega = 0$ or $\boldsymbol{h} = \lambda\omega$ ($\lambda \neq 0$). The equilibrium with $\omega = 0$ is the desired state, so that we can ignore it. From (B13), therefore, one obtains

$$(J_t - \lambda)\omega_s = -I_{ws}\Omega \qquad (B14)$$

$$(J_a - \lambda)\omega_g = 0 \qquad (B15)$$

The case with $\omega_g = 0$ has been examined already, so that we only need to check the case $\lambda = J_a$. For this case, it is easy to show that

$$\omega_s = \frac{H_0}{J_a - J_t - I_{ws}^2/k_\Omega} \qquad (B16)$$

and

$$\omega_g = \pm \sqrt{H_0^2\left[\frac{1}{J_a^2} - \frac{1}{(J_a - J_t - I_{ws}^2/k_\Omega)^2}\right]} \qquad (B17)$$

where we have used the fact that $\Omega = \Omega_e^+ + \Omega_f^+ = I_{ws}\omega_s/k_\Omega + H_0/I_{ws}$ and $\| \boldsymbol{h} \| = H_0$. This equilibrium state correspond to column E3 in Table 1. Note that this equilibrium is possible only when $2J_a - J_t - I_{ws}^2/k_\Omega \leq 0$.

Acknowledgement

References

[1] Aeyels, D., and Szafranski, M., "Comments on the Stabilizability of the Angular Velocity of a Rigid Body," *Systems & Control Letters*, Vol. 10, No. 1, 1988, pp. 35–39.

[2] Sontag, E., and Sussmann, H., "Further Comments on the Stabilizability of the Angular Velocity of a Rigid Body," *Systems & Control Letters*, Vol. 12, No. 3, 1989, pp. 213–217.

[3] Andriano, V., "Global Feedback Stabilization of the Angular Velocity of a Symmetric Rigid Body," *Systems & Control Letters*, Vol. 20, No. 5, 1993, pp. 361–364.

[4] Morin, P., "Robust Stabilization of the Angular Velocity of a Rigid Body with Two Controls," *European Journal of Control*, Vol. 2, 1996, pp. 51–56.

[5] Tsiotras, P., and Schleicher, A., "Detumbling and Partial Attitude Stabilization of a Rigid Spacecraft Under Actuator Failure," AIAA Paper 00-4044, 2000.

[6] Byrnes, C. I., and Isidori, A., "On the Attitude Stabilization of a Rigid Spacecraft," *Automatica*, Vol. 27, No. 1, 1991, pp. 87–95.

[7] Krishnan, H., Reyhanoglu, M., and McClamroch, H., "Attitude Stabilization of a Rigid Spacecraft Using Two Control Torques: A Nonlinear Control Approach Based on the Spacecraft Attitude Dynamics," *Automatica*, Vol. 30, No. 6, 1994, pp. 1023–1027.

[8] Tsiotras, P., Corless, M., and Longuski, M., "A Novel Approach to the Attitude Control of Axisymmetric Spacecraft," *Automatica*, Vol. 31, No. 8, 1995, pp. 1099–1112.

[9] Coron, J. M., and Keraï, E. L., "Explicit Feedback Stabilizing the Attitude of a Rigid Spacecraft with Two Control Torques," *Automatica*, Vol. 32, No. 5, 1996, pp. 669–677.

[10] Morin, P., and Samson, C., "Time-Varying Exponential Stabilization of a Rigid Spacecraft with Two Control Torques," *IEEE Transactions on Automatic Control*, Vol. 42, No. 4, 1997, pp. 528–534.

[11] Spindler, K., "Attitude Control of Underactuated Spacecraft," *European Journal of Control*, Vol. 6, No. 3, 2000, pp. 229–242.

[12] Tsiotras, P., and Luo, J., "Stabilization and Tracking of Underactuated Axisymmetric Spacecraft with Bounded Inputs," *Automatica*, Vol. 36, No. 8, 2000, pp. 1153–1169.

[13] Tsiotras, P., and Doumtchenko, V., "Control of Spacecraft Subject to Actuator Failures: State-of-the-Art and Open Problems," *Journal of the Astronautical Sciences*, Vol. 48, No. 2, 2000, pp. 337–358.

[14] Krishnan, H., McClamroch, H., and Reyhanoglu, M., "Attitude Stabilization of a Rigid Spacecraft Using Two Momentum Wheel Actuators," *Journal of Guidance, Control, and Dynamics*, Vol. 18, No. 2, 1995, pp. 256–263.

[15] Kim, S., and Kim, Y., "Spin-Axis Stabilization of a Rigid Spacecraft Using Two Reaction Wheels," *Journal of Guidance, Control, and Dynamics*, Vol. 24, No. 5, 2001, pp. 1046–1049.

[16] Vadali, S. R., and Junkins, J. L., "Spacecraft Large Angle Rotational Maneuvers with Optimal Momentum Transfer," *Journal of the Astronautical Sciences*, Vol. 31, No. 2, 1983, pp. 217–235.

[17] Hall, C., "Momentum Transfer in Two-Rotor Gyrostats," *Journal of Guidance, Control, and Dynamics*, Vol. 19, No. 5, 1996, pp. 1157–1161.

[18] Bang, H., Myung, H.-S., and Tahk, M.-J., "Nonlinear Momentum Transfer Control of Spacecraft by Feedback Linearization," *Journal of Spacecraft and Rockets*, Vol. 39, No. 6, 2002, pp. 866–873.

[19] Ford, K. A., and Hall, C. D., "Flexible Spacecraft Reorientations Using Gimbaled Momentum Wheels," *Advances in the Astronautical Sciences, Astrodynamics*, edited by F. Hoots, B. Kaufman, P. J. Cefola, and D. B. Spencer, Vol. 97, Univelt, San Diego, 1997, pp. 1895–1914.

[20] Junkins, J. L., and Schaub, H., "Feedback Control Law for Variable Speed Control Moment Gyroscopes," *Journal of the Astronautical Sciences*, Vol. 46, No. 3, 1998, pp. 307–328.

[21] Schaub, H., and Junkins, J. L., "Singularity Avoidance Using Null Motion and Variable-Speed Control Moment Gyros," *Journal of Guidance, Control, and Dynamics*, Vol. 23, No. 1, 2000, pp. 11–16.

[22] Yoon, H., and Tsiotras, P., "Spacecraft Adaptive Attitude and Power Tracking with Variable Speed Control Moment Gyroscopes," *Journal of Guidance, Control, and Dynamics*, Vol. 25, No. 6, Nov.–Dec. 2002, pp. 1081–1090.

[23] Yoon, H., and Tsiotras, P., "Singularity Analysis of Variable-Speed Control Moment Gyros," *Journal of Guidance, Control, and Dynamics*, Vol. 27, No. 3, 2004, pp. 374–386.

[24] Marshall, A., and Tsiotras, P., "Spacecraft Angular Velocity Stabilization Using a Single-Gimbal Variable Speed Control Moment Gyro," AIAA Paper 03-5654, 2003.

[25] Richie, D. J., Tsiotras, P., and Fausz, J. L., "Simultaneous Attitude Control and Energy Storage Using VSCMGs : Theory and Simulation," *Proceedings of American Control Conference*, Vol. 5, Institute of Electrical and Electronics Engineers, Piscataway, NJ, 2001, pp. 3973–3979.

[26] Kailath, T., *Linear Systems*, Prentice–Hall, Englewood Cliffs, New Jersey, 1980, pp. 135–139.

[27] Tsiotras, P., Yoon, H., and Marshall, A., "Controllability Analysis and Control of Spacecraft Using a Single-Gimbal Variable-Speed Control Moment Gyroscope," Internal Report, School of Aerospace Engineering, Georgia Institute of Technology, Atlanta, GA, January 2004.

[28] Zhou, K., Doyle, J., and Glover, K., *Robust and Optimal Control*, Prentice–Hall, New Jersey, 1996.

[29] Hughes, P. C., *Spacecraft Attitude Dynamics*, John Wiley & Sons, New York, 1986.

[30] Sidi, M. J., *Spacecraft Dynamics and Control*, Cambridge University Press, Cambridge, UK, 1997.